



NTNU – Trondheim
Norwegian University of
Science and Technology

Analytical & Numerical Analysis of Ship/FPSO Side Structures Subjected to Extreme Loading with Emphasis of Ice Actions

Md Habibullah Bahar

Marine Technology

Submission date: June 2014

Supervisor: Jørgen Amdahl, IMT

Co-supervisor: Havard Nyseth, DNV-GL

Norwegian University of Science and Technology
Department of Marine Technology



NTNU – Trondheim
Norwegian University of
Science and Technology

Master Thesis

Spring 2014

**Analytical & Numerical Analysis of Ship/FPSO
Side Structures Subjected to Extreme Loading
with Emphasis of Ice Actions**

Md Habibullah Bahar

Department of Marine Technology

Supervisor: Jørgen Amdahl, IMT

Submission date: June 2014

Abstract

IACS has implemented a unified requirement (UR) for polar going ships. This thesis work consists of a well understanding of the backgrounds of IACS UR, the way of applying those rules to the structure and the comparison of different requirements among different polar classes indicated in IACS. Average ice load, design ice load patch dimensions are calculated for different ship size. This thesis includes a better perception about plastic collapse mechanism method which is the main principle of IACS framing requirements.

A DNV class FPSO had been chosen to apply the IACS requirements and it has brought a comparative view between IACS with a non IACS class ship. Two different simplified collapse mechanism models have been developed for a single longitudinal frame of the FPSO concerned. Moreover using Abaqus, a non-linear finite element analysis has been performed for a large part of side plating of that FPSO. Then, twice elastic slope method is used to establish limit load from analysis result. By observing limit loads and combining with them with IACS UR, an argument has been drawn regarding validity of this FPSO according to IACS Polar Class.



Scope of work

The DNV management team has identified Arctic Operation and Technology as one of the main strategic focus areas. Transport and exploitation of resources in the Northern areas are increasingly focused upon. The corresponding climatic conditions represent a challenge both to the operation and design of ships in these waters. The presence of sea ice is the main factor hindering operations in the Arctic. Sea ice is a complex material and induces high pressures when being in contact with ships or structures. In order to understand the nature of the associated forces, the ice physics and ice mechanics have to be studied.

The intention of this work is to obtain a basic understanding of the physics involved in ship ice interaction and to be updated on current activities related to the topics.

The Thesis work shall address the following topics:

1. Review of IACS Polar Class (UR I1) requirements from PC1 to PC7 PC 2/3/4/5
2. Compare the different requirements for structural design for each ice class. Discuss the differences between the various classes with respect strength. How are these differences implemented in the rules and what is the most crucial parameters that impose these steps in the rules. Compare the different methods for estimation of ice pressure for each ice class
3. Comment on the above mentioned theory study with respect to the validity of using these methods for the design of a moored Arctic FSPO/driller
4. Determine the required plate thickness and stiffener dimensions for a range of stiffener spacing and length.
5. Perform nonlinear finite element analysis of a single frame subjected to ice patch loading. Compare the results with the models underlying the IACS polar code.
6. To the extent that local buckling occurs in the web plate of the web frame, propose additional secondary stiffening and verify their effect by performing NLFEA.



7. Perform analysis of a large part of the ship side, containing stiffeners, web frames and stringers. Discuss in particular how boundary conditions have been modeled. Perform NLFEA and identify primary collapse mechanisms. Compare the results with simplified capacity models. On the basis of the simulations assess limit loads when fracture in the plating is likely to take place. The distribution of pressure loads is to be determined in agreement with the supervisor.

8. To the extent time permits perform modeling and analysis of a bow panel. Compare the results with simplified methods

9. Conclusions and recommendations for further work

Preface

This thesis has been done for the partial fulfilment of the requirements for Master of Science degree program at the department of Marine Technology, Norwegian University of Science and Technology (NTNU), Trondheim, Norway.

This thesis is accomplished in spring 2014. In the time frame of thesis, the analysis for the bow section had to be omitted and work of verifying the IACS rules for moored FPSO had been limited to only basic concepts in consultation with my supervisor Professor Jørgen Amdhal.

I would like to express my gratitude to my honorable supervisor Professor Jørgen Amdhal for his advice, guidance and continuous support through this thesis.

It is a pleasure to thank Martin Storheim and Katerina kim for helping me on Abaqus. I like to offer my regards and blessings to my friend Oystein Helland, Mohammad Irfan Uddin and other friends for sharing their thoughts regarding my projects.

Trondheim, 10th of June 2014

Md Habibullah Bahar

Table of Contents

Abstract	i
Scope of work	iii
Preface	v
Table of Contents	vi
Table of Figures	ix
List of Tables	xi
Nomenclature	xii
Introduction	1
1. Review of IACS Polar Class Requirements.....	2
1.1. Polar Classes.....	2
1.2. Upper and Lower Ice waterlines.....	4
1.3. Hull Areas.....	4
1.4. Design Ice Load.....	5
1.5. Design Load Patch.....	9
1.6. Peak Pressure Factor (PPF).....	12
1.7. IACS Structural Requirements	13
1.7.1. Membrane effect	13
1.7.2. Energy Method.....	14
1.7.3. Collapse Mechanism	14
1.7.4. Moment and shear interaction.....	17
1.7.5. Collapse mechanisms in IACS requirements.....	18
1.7.6. Centrally loaded patch	19
1.7.7. End load case (Asymmetric load).....	23
2. Comparison of Polar Classes.....	25
2.1. Ice load	25
2.2. Framing Requirements.....	29
2.2.1. Shell plate requirements	29



2.2.2. Shear Area.....	30
3. IACS UR for a moored Arctic FPSO.....	32
4. Assessment of a FPSO.....	34
5. Non-linear finite element analysis of a single frame.....	38
5.1. Non-Linear Finite Element Analysis.....	39
5.2. Finite element model.....	40
5.3. Material Property.....	40
5.4. Boundary Condition.....	41
5.5. Load.....	44
5.6. Analytical Formulas.....	45
5.7. Analytical Results.....	48
5.8. Abaqus Results.....	48
6. Analysis of a large part of the ship side.....	51
6.1. Boundary conditions.....	52
6.2. Loading.....	53
6.3. Meshing Technique.....	54
6.4. Abaqus analysis result.....	55
6.4.1. Comparing boundary condition.....	55
6.4.2. Material comparison.....	56
6.4.3. Result of whole structure at different positions.....	57
6.4.4. Comparison between whole structure and single longitudinal results 59	
6.4.5. Introducing additional stiffeners.....	60
6.5. Assessing limit loads.....	60
6.5.1. Twice elastic slope method.....	61
6.5.2. Tangent Intersection Method.....	61
6.5.3. Limit Loads.....	62
7. Conclusions.....	65
8. Recommendation for further work.....	67
Bibliography.....	69



A. Appendix.....	i
Matlab script	i
Provided Drawings.....	iii
Plots	v
Calculations	vii

Table of Figures

Figure 1-1: Comparison of ice classes by nominal ice thickness [5].....	3
Figure 1-2: Hull area extent [1]	4
Figure 1-3: Pressure variance as Hull Area variation [6]	5
Figure 1-4: Design scenario – Glancing scenario and flexural failure [3].....	6
Figure 1-5: Ice collision geometry with an ice edge [3]	6
Figure 1-6: Ice crush till flexural strength of ice.....	7
Figure 1-7: Hull Angles [1]	8
Figure 1-8: Ice Failure Mode [7]	9
Figure 1-9: Nominal and design rectangular load patches [3]	10
Figure 1-10: Ice load patch configuration [3].....	10
Figure 1-11: Ice Failure including crashing and spalling [7]	11
Figure 1-12: Peak Pressure Factor to design individual elements [3].....	12
Figure 1-13: Load-deflection curves including membrane effect [9] [10].....	14
Figure 1-14: Formation of 3-hinge collapse mechanism for uniformly loaded beam	16
Figure 1-15: load development and material behavior during formation of 3-hinge	17
Figure 1-16: Shear-Moment interaction [11]	17
Figure 1-17: Simplified Plastic Modulus concept [11]	19
Figure 1-18: Cross section dimensions as defined by IACS [1]	19
Figure 1-19: 3-hinge Collapse Mechanism for centrally patch loaded frame with fixed-fixed ends	20
Figure 1-20: End loaded fixed-fixed frame, with assumed plastic mechanism ..	23
Figure 2-1: Ice load parameter dependency on hull area	25
Figure 2-2: Class factor variations.....	27
Figure 2-3: Pressure variance for different displacement	28
Figure 2-4: Load Patch dimension variations	28
Figure 2-5: Thickness variations.....	30
Figure 2-6: Thickness variation as frame spacing changes.....	30
Figure 2-7: Min shear area requirements as IACS.....	31
Figure 3-1: Ice vanning: Ice drifts and ship direction [12]	32
Figure 4-1: Parameter Definition for Web Stiffening [1]	37
Figure 5-1: Single Frame selection	38
Figure 5-2: Non-linear behavior of a thin plate/shell [15].....	39
Figure 5-3: Typical unstable response of structure [16]	40

Figure 5-4: Elastic-Purly plastic material behavior	41
Figure 5-5: Single Longitudinal (First Phase)	42
Figure 5-6: Single Longitudinal (Final Phase).....	42
Figure 5-7: Boundary Condition for single Longitudinal Frame.....	43
Figure 5-8: Displacement pattern in whole grillage part at 1.5MPa load	44
Figure 5-9: Loading of Single longitudinal frame.....	44
Figure 5-10: Single frame 1 st model	45
Figure 5-11: 2 nd Collapse Mechanism for single longitudinal frame	46
Figure 5-12: Pressure vs. Deformation plot single longitudinal with span of 4.43m (case1)	49
Figure 5-13: Pressure vs. Deformation plot for individual longitudinal at centre.	49
Figure 5-14: Deformation of longitudinal at 1.4 MPa load.....	50
Figure 5-15: Shear Stress in 1.4MPa.	50
Figure 6-1: Side Structure Abaqus model.....	51
Figure 6-2: Load transfer hierarchy.....	52
Figure 6-3: Boundary condition for plate edge in longitudinal direction	53
Figure 6-4: Loading on a large side part	54
Figure 6-5: Meshing of the model.....	55
Figure 6-6: Mesh in loading area.....	55
Figure 6-7: Deformation difference between two boundary conditions	56
Figure 6-8: Plasticity effect on Abaqus result	57
Figure 6-9: Load-deformation plot of whole grillage, at many points.....	57
Figure 6-10: Deformation contour plot in 1.7MPa load (showing points for plots in Figure 6-9)	58
Figure 6-11: Load-Deformation plot for longitudinal (single and in whole structure)	59
Figure 6-12: Load-Deformation plot for modified grillage	60
Figure 6-13: Twice elastic slope method [19].....	61
Figure 6-14: Tangent Intersection Method.....	62
Figure 6-15: Limit load for 3-hinge mechanism	62
Figure 6-16: Determining Limit Load.....	63
Figure 6-17: Limit loads for web with additional stiffener.....	64
Figure 6-18: Deformation plot of modified grillage.....	64
Figure 8-1: Deformation of single longitudinal	67
Figure 8-2: 3 rd collapse mechanism for longitudinal frame.....	68
Figure A-1: Drawing of Web frame.....	iii

Figure A-2: Drawing of Ordinary web frame.....	iii
Figure A-3: Modified grillage model	iv
Figure A-4: Displacement contour plot of longitudinal	v
Figure A-5: Deformation at 2.1MPa load.....	v
Figure A-6: Deformation contour plot for BC1 and BC2 at 2MPa load.....	vi
Figure A-7: Stress contour plot for BC1 and BC2 in 2MPa load	vi
Figure A-8: Deformation at 3.3MPa load.....	vii

List of Tables

Table 1: Polar Classes [1]	2
Table 2: Class factors [1]	26
Table 3: Principle particulars of the FPSO	34
Table 4: Side Structure Dimension details	35
Table 5: IACS calculated values for 186.12 KT displacements FPSO	35



Nomenclature

ABS	American Bureau of Shipping
Af	Stiffener Flange Area
A_w	Stiffener Web area
AR	Aspect ratio
b	Patch load height
BC	Boundary Condition
b_w, Wf, bf	Width of stiffener flange
CASPER	Canadian Arctic Shipping Pollution Prevention Regulation
C_o	Mass reduction coefficient
CF_c	Crushing class factor
CF_D	Patch class factor
CF_F	Flexural class factor
D_{ship}	Ship displacement
KT	kilo ton
E_{crush}	Ice crushing energy
FPSO	Floating Production Storage and Offloading
FSR	Finish-swedish rules
F_n	Normal force
hw	Stiffener web height
h_{ice}, h_i	Ice thickness
h_{fc}	Height of stiffener measured to the center of the flange area
KI	Tangent stiffness or increment stiffness
Ken	Normal Kinetic Energy
L	frame length
M	Bending moment
M_e	effective mass
M_p	Plastic bending moment
M_{pr}	Reduced Plastic bending moment
M_{ship}	Ship mass
M_{pw}	Bending moment at mid-span in the flange
NLFEM	Non-Linear Finite Element analysis
P	Class dependent ice pressure
P_{3h}	IACS UR limit state load for 3 hinge collapse
Q	Line load
S, s	Stiffener spacing
T	Shear



TES	Twice Elastic Slope
tf	Flange thickness
tp	Plate thickness
tw	Stiffener web thickness
UR	IACS unified requirement
U _x	Translation in x direction
U _y	Translation in y direction
U _z	Translation in z direction
UR _x	Rotation about x axis
UR _y	Rotation about y axis
UR _z	Rotation about z axis
V _{ship}	Ship velocity
V _n	normal velocity
Z, Z _p	Plastic section modulus
Z _w	Plastic section modulus of stiffener web
σ	stress
σ _f , σ _y	Yield stress
ε	strain
δ	Normal ice penetration, deflection
φ _w	Angle between the shell plate and the flange side of web



Introduction

Transportation and exploitation of resources are increasing in the Northern area day by day. The climate of arctic area is the major challenging factor. The ships which are trading in arctic area, has to face the presence of ice. Ice is a complex material and creates high pressure during contact with ship and structures. So, well understanding the ice load on structure is the main factor to take into account for designing a ship for arctic area.

To mitigate this challenge International Association of Classification Societies combining with other classification societies has formed a Unified Requirements (UR). Understanding the principles, methods used and the way of derivation of the formulations described in IACS UR, 2011 [1] are the main inspirations of this thesis work. IACS requirements differ with 7 different polar class; PC1 to PC7 (Table 1) according to ship owner trading purpose and operational window. Ice load, framing requirements vary among these seven polar classes.

To get a comparative assessment, a FPSO has been chosen under DNV class, named 'White Rose Field Husky Oil FPSO'. Method behind DNV polar class requirements is different than IACS. DNV used elastic method [2] to derive their formulas but IACS has used plastic method. Plastic method allows large deflection and post ultimate resistance range which utilize the overloading concept which is common fact nowadays. Plastic methods are normally applied where the load are extreme and not cyclic in nature which is so much in line with ice load nature. Ice load nature is different for a moored structure and that's why it is also a concern to verify the IACS UR for that situation.

Finite Element Method is a popular numerical technique for engineering analysis. Adding non-linear behaviour to this method is a good choice when we need ultimate strength of structure which can buckle as well. In this work geometrical and material non-linearity has been considered. Abaqus is a powerful tool to perform non-linear finite element analysis and reliable to take as a real analysis value. So IACS requirements comparison with Abaqus results can give a satisfactory assessment for our regarding structure.

1. Review of IACS Polar Class Requirements

An international committee including representatives from many classification societies and polar nations developed requirements concerning polar class in the form of a Unified Requirement, International Association of Classification Society (IACS) standard. IACS standards are applicable to steel made ships which are desired to navigate in ice-surrounded polar waters, except ice breakers [1]. IACS unified requirements differs when the ice condition varies. Ice formation is complex and it is the main challenge to estimate the ice load perfectly. Daley shows the approach to determine the ice load in his paper [3] for IACS and the rules are based on single frame loading. Framing requirements are described in the paper of Daley and Kendrick [4], are based on plastic collapse mechanism work-energy principle. The different feature, backgrounds behind ice load calculation and framing requirements including some comparison with other classification societies are described below:

1.1. Polar Classes

Designing of a ship for operating in polar area, it is must to know about the ice condition in that route, duration of ice extent, operation window for that ship etc. Considering these issues IACS unified rules are classified into 7 polar classes. These Polar classes are the notation for making differences among the requirements of polar ships with respect to strength and operational window. Ships that comply with the IACS UR can be considered for a Polar class notation as listed in Table 1

Table 1: Polar Classes [1]

Polar class	Ice Description(Based on WMO Sea Ice Nomenclature)
PC 1	Year-round operation in all Polar waters
PC 2	Year-round operation in moderate multi-year ice conditions
PC 3	Year-round operation in second-year ice which may include multiyear ice inclusions.
PC 4	Year-round operation in thick first-year ice which may include old ice inclusions

PC 5	Year-round operation in medium first-year ice which may include old ice inclusions
PC 6	Summer/autumn operation in medium first-year ice which may include old ice inclusions
PC 7	Summer/autumn operation in thin first-year ice which may include old ice inclusions

Owner selects an appropriate polar class and this selection keep that ship in balance with strength to ice condition keeping the economic consideration in mind.

We can get an idea how IACS polar classes differ with other classification societies with respect to nominal ice thickness (Figure 1-1) [5]

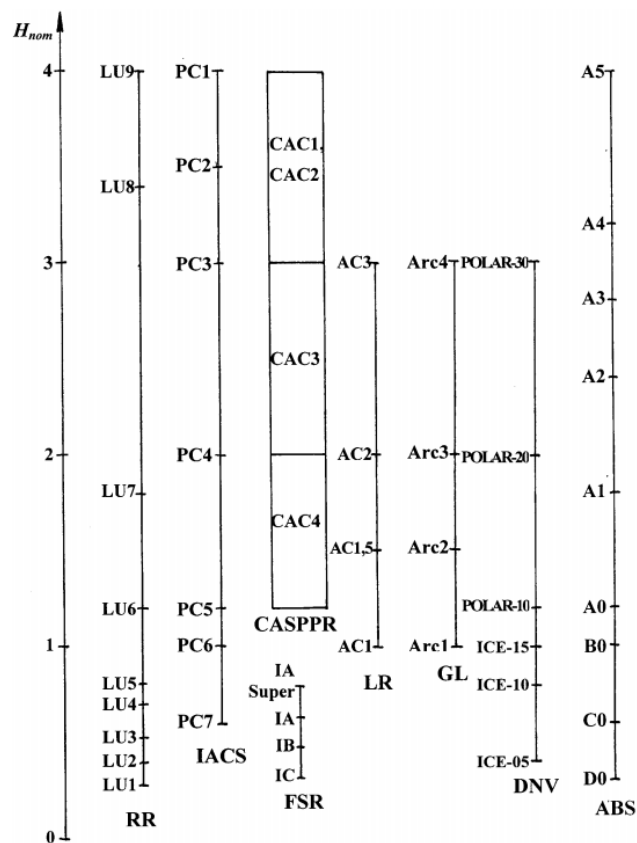


Figure 1-1: Comparison of ice classes by nominal ice thickness [5]

From ice thickness comparison IACS classes are different from every class. The higher class limit is same with Canadian arctic shipping regulations, Russian

Register and ABS. The lightest class PC 7 of IACS is in between ICE-05 and ICE-10 of DNV class. The highest polar class of DNV, Polar 30 is equivalent to IACS PC4.

1.2. Upper and Lower Ice waterlines

The upper ice waterline (UIWL) is the maximum draughts fore, amidships and aft. The lower ice waterline is the minimum draughts fore, amidships and aft. The lower ice waterline is determined in ballast condition so that propeller submerges.

1.3. Hull Areas

The hull of polar class ships is divided into areas according to the expected load act upon them.

There are four regions:

- | | | |
|--------------------|---|--------------------|
| • Bow | } | • Bottom |
| • Bow intermediate | | • Lower |
| • Mid-body | | • Ice belt regions |
| • Stern | | |

This can be illustrated as following figure.

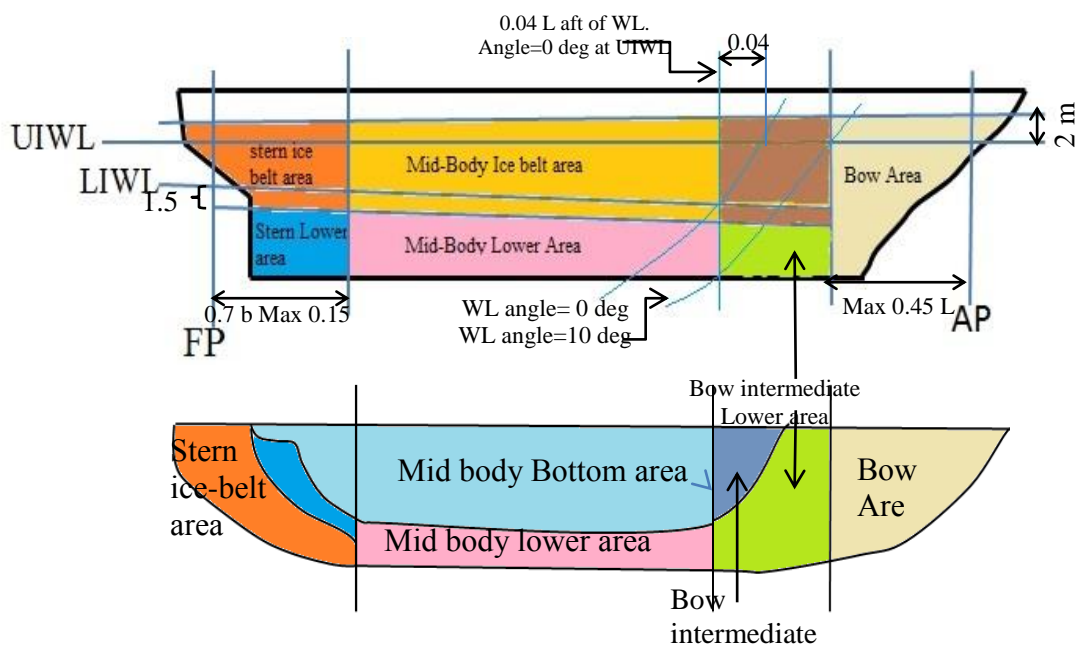


Figure 1-2: Hull area extent [1]

Hull area is divided into many portions as the requirements vary on hull area as the ice load is not same in all areas. The bow area faces the highest forces and lowers for other portions. A typical pressure variation is shown below as hull area described in Figure 1-2.

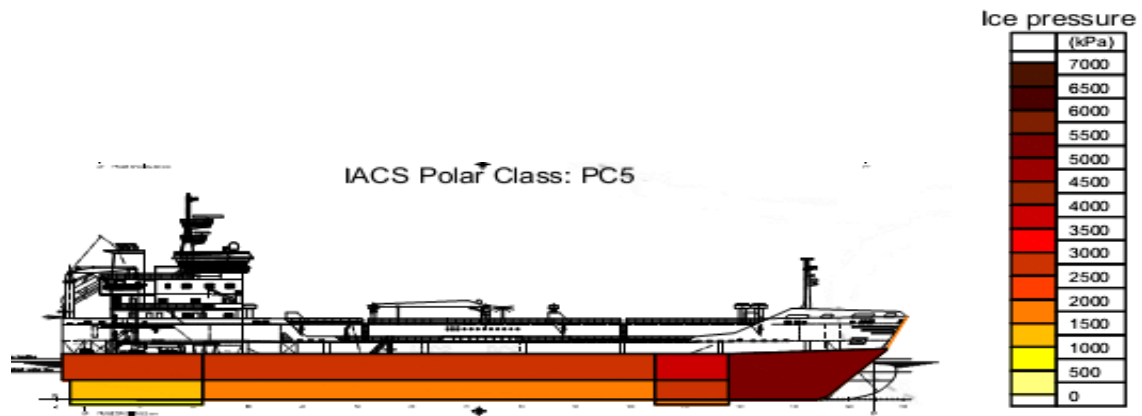


Figure 1-3: Pressure variance as Hull Area variation [6]

1.4. Design Ice Load

Ice load is established based on a design scenario and it is a glancing collision with an ice edge (Figure 1-4). This scenario is linked to the ice load with a ratio. Ice load equations are based on energy based collision model and this model assumes a ‘Popov’ type of collision in which ice indentation is introduced by a pressure area relationship. The following derivation process is based on as described in ‘Annex’ of paper of (Daley 2000) [3].

The following are considered for solving the ice load equation:

- Ice thickness
- Ice strength(crushing pressures)
- Hull form
- Ship size
- Ship speed

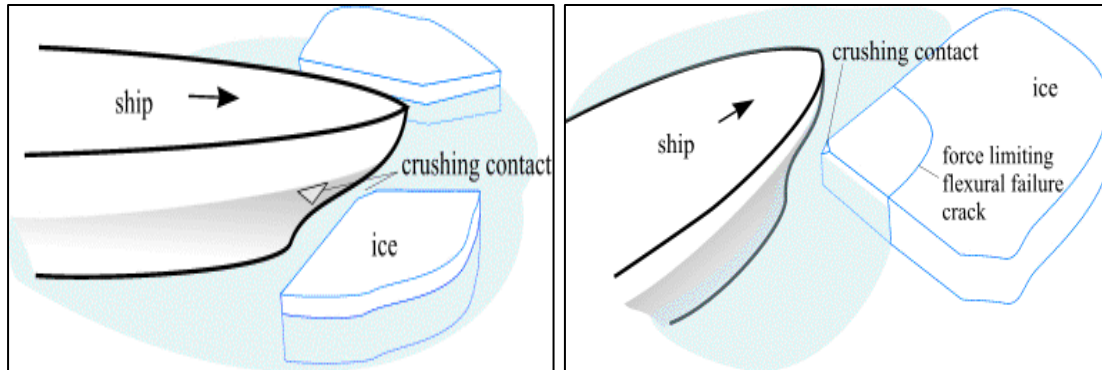


Figure 1-4: Design scenario – Glancing scenario and flexural failure [3]

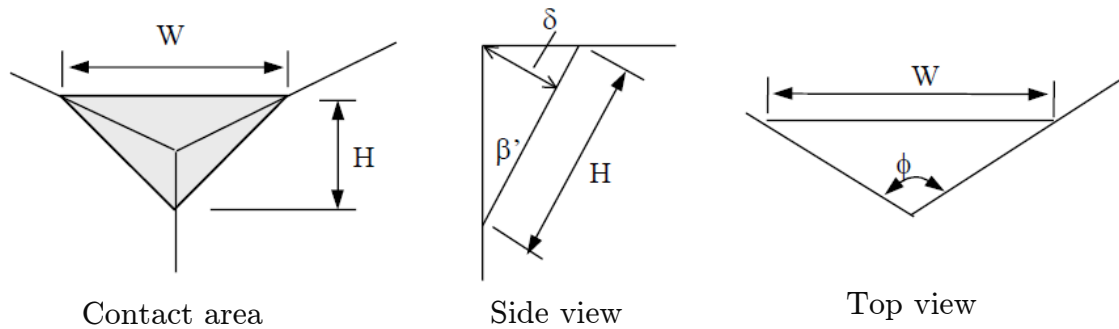


Figure 1-5: Ice collision geometry with an ice edge [3]

In this glancing scenario, it is assumed that a ship is in her design speed strikes an angular ice edge and she penetrates the ice and rebounds away. Then ice force is determined by equating the normal kinetic energy and ice crushing energy over penetration depth,

$$\frac{1}{2} M_e V_n^2 = \int_0^{\delta} F_n(\delta) \cdot d\delta \quad (1-1)$$

Where,

- δ = normal ice penetration
- F_n = normal force
- M_e = effective mass = M_{ship}/Co
- V_n = normal velocity = $V_{ship} l$
- l = direction cosine

Using the ice penetration geometry (Figure 1-5) combining with pressure-area relationship, ice crushing normal force has been calculated. The maximum ice crushing force cannot be higher than the force to fail the ice in bending (Figure 1-6). Limit force for bending is defined by the combination of angles, ice strength and thickness (see equation 1-8).

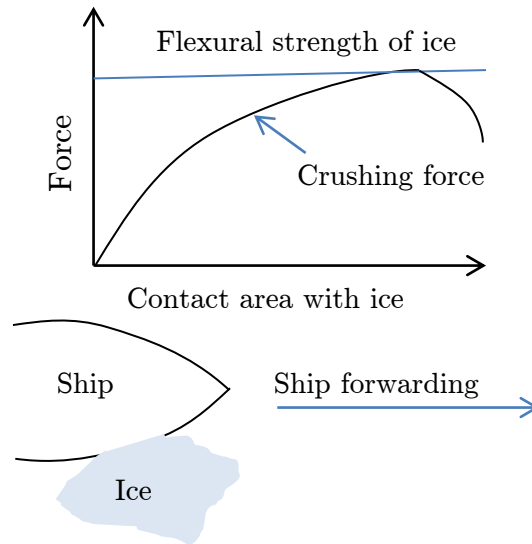


Figure 1-6: Ice crush till flexural strength of ice

The nominal contact area from Figure 1-5,

$$A = \frac{W}{2} H \quad (1-2)$$

Where,

$$W = \frac{2\delta \tan\left(\frac{\phi}{2}\right)}{\cos \beta'} \quad (1-3)$$

$$H = \frac{\delta}{\sin \beta' \cos \beta'} \quad (1-4)$$

Now, average pressure is determined by pressure area relationship,

$$P = P_0 A^{\text{ex}} \quad (1-5)$$

Where, P_0 is a class dependent ice pressure at 1 m^2 [MPa].

Then after some calculation we get the normal ice load, (details calculation in Appendix of the paper of Daley [3])

$$F_n = (3 + 2 \cdot ex)^{\frac{2+2 \cdot ex}{3+2 \cdot ex}} \cdot P_0^{\frac{1}{3+2 \cdot ex}} \cdot \left(\frac{\tan(\phi/2)}{\sin \beta' \cos^2 \beta'} \right)^{\frac{1+ex}{3+2 \cdot ex}} \cdot \left(\frac{1}{2} \Delta_n \cdot V_n^2 \right)^{\frac{2+2 \cdot ex}{3+2 \cdot ex}} \quad (1-6)$$

Where, $\Delta_n = \frac{\Delta_{ship}}{C_0}$

Here in this equation, ex connects the force solution with the pressure-area relationship. Only the ice pressure at 1 m² P_0 is a class dependent parameter. Other variables are the hull angles (Figure 1-7) and ship displacement. So the force is dependent on ship bow shape and ship size.

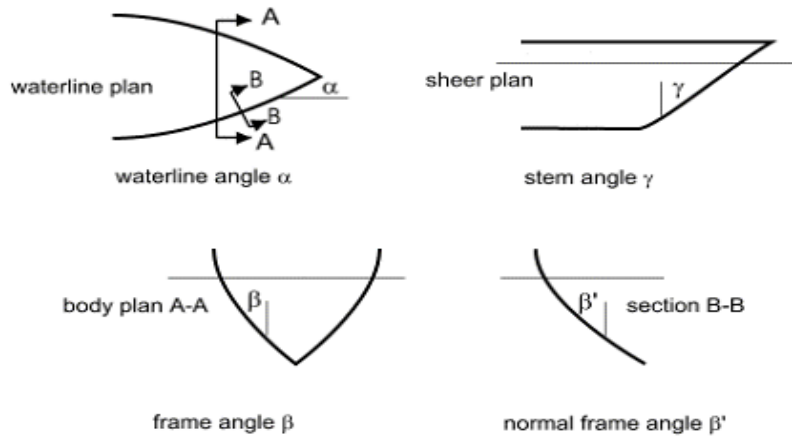


Figure 1-7: Hull Angles [1]

Equation (1-6) can be simplified by following equation by taking $ex=-0.1$, $\phi=150$ deg and collecting the all the angle term into fa by following,

$$F_n = fa \cdot P_0^{0.36} \cdot \Delta_{ship}^{0.64} \cdot V_{ship}^{1.28} \quad (1-7)$$

Where, shape coefficient fa is,

$$fa = \text{minimum_of} \left\{ \begin{array}{l} \left(0.097 - 0.68 \left(\frac{x}{L} - 0.15 \right)^2 \right) \frac{\alpha}{\sqrt{\beta'}} \dots \text{crushing_failure} \\ \frac{1.2CF_F}{\sin \beta' \cdot CF_C \cdot \Delta_{ship}^{0.64}} \dots \text{Flexural_failure} \\ 0.60 \dots \text{Limiting_value} \end{array} \right. \quad (1-8)$$

Where,

x = distance from forward perpendicular to the station under consideration

CF_F = Flexural Class factor = $\sigma_f h_{ice}^2$

CF_C = Crushing class factor = $P_0^{0.36} \cdot V_{ship}^{1.28}$

h_{ice} = ice thickness [m] [class dependent]

σ_f = ice flexural strength [Mpa] [class dependent]

β' = normal (true) frame angle

In equation (1-8) fa has been considered for different failure mode of ice (Figure 1-8) and the minimum value has to be considered to calculate the ice load. By introducing flexural failure, the crushing load is now limited up to flexural failure. Crushing failure load cannot be higher than the flexural failure load. For crushing failure fa measured at several locations at the bow area to find the dimensioning load. The maximum value of fa is bound to be within 0.6 for avoiding extreme value. Finally, the minimum value has to be taken.

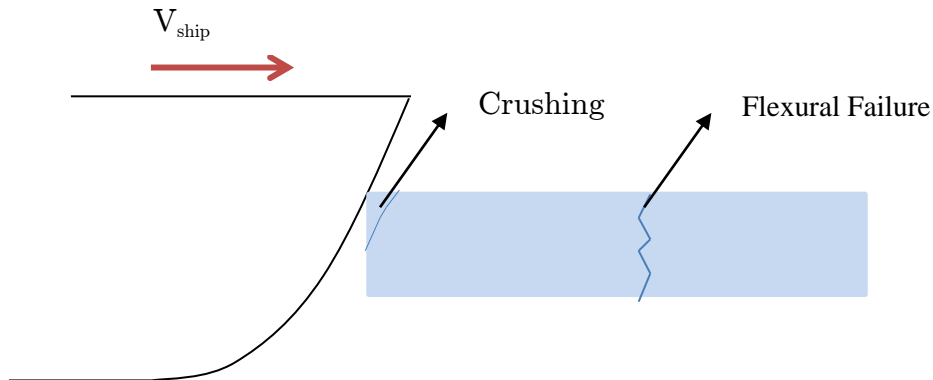


Figure 1-8: Ice Failure Mode [7]

After introducing the class factors, the load equation (1-7) be simplified to,

$$F_n = fa \cdot CF_C \cdot \Delta_{ship}^{0.64} \quad (1-9)$$

1.5. Design Load Patch

From the equation (1-5), it can be said that ice force has a relation with nominal contact area between ship and ice. This contact area (nominal-overlapped) then simplified from triangular to an equivalent area rectangular patch which is called design load patch and the average pressure is distributed

uniformly over the area patch. Then this ice load patch is reduced to be conservative by taking account the ice edge spalling effect (Figure 1-11).

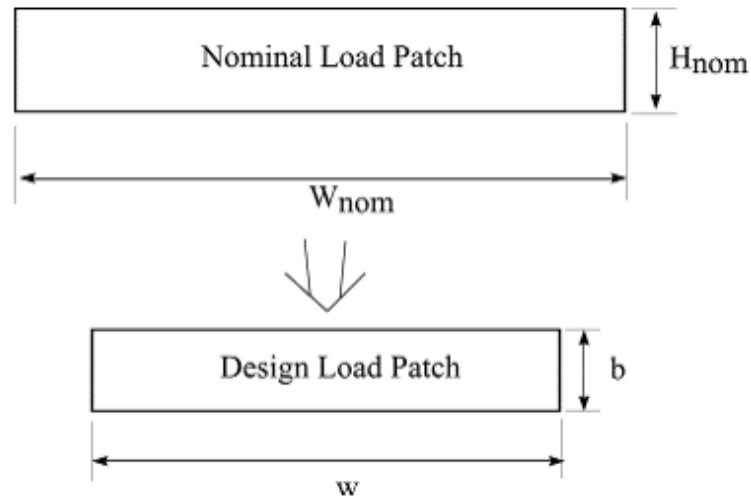


Figure 1-9: Nominal and design rectangular load patches [3]

Then we get the simplified design load patch with height b and width w as shown in Figure 1-10.

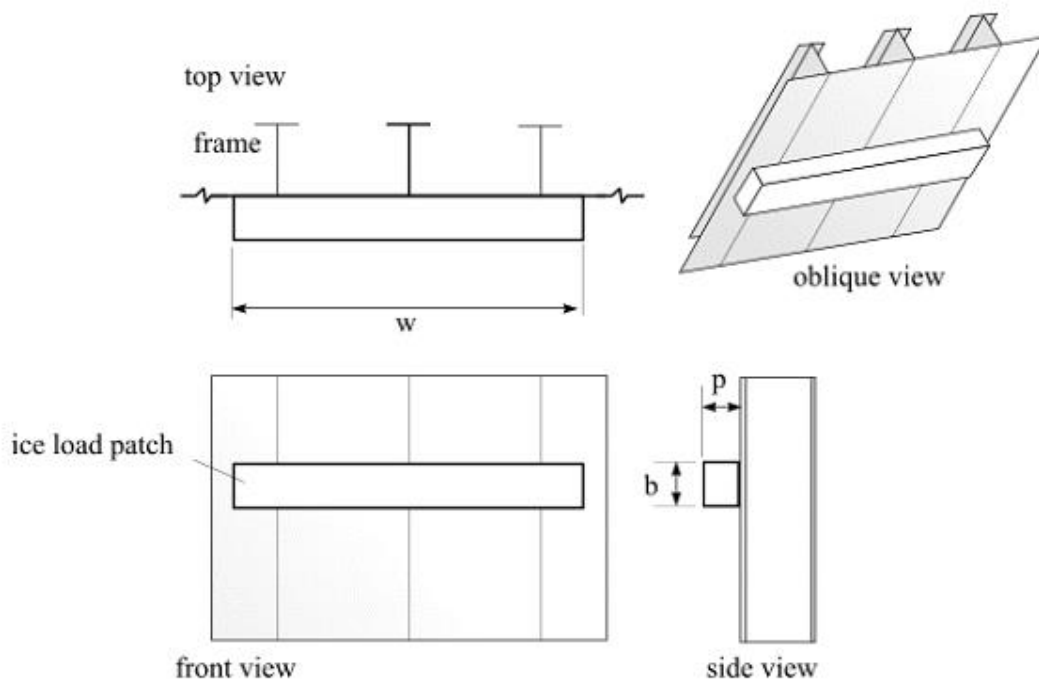


Figure 1-10: Ice load patch configuration [3]

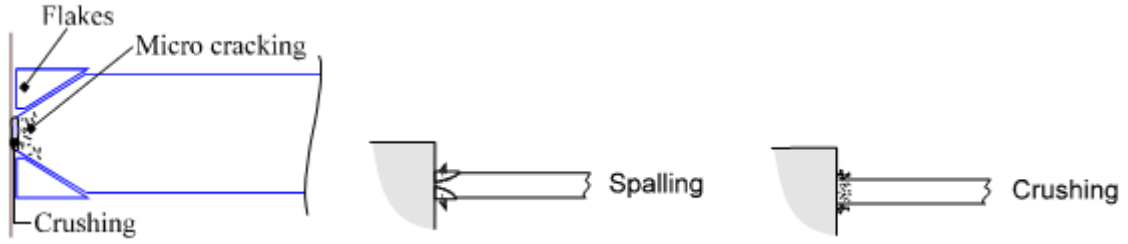


Figure 1-11: Ice Failure including crushing and spalling [7]

So as described in Figure 1-9, the area of the nominal load patch using area pressure relationship will be (combining with equation 1-5)

$$A_{nom} = H_{nom} \cdot W_{nom} = \left(\frac{F_n}{P_0} \right)^{\frac{1}{1+ex}} \quad (1-10)$$

Introducing aspect ratio,

$$AR = \frac{W_{nom}}{H_{nom}} \quad (1-11)$$

Using equation 1-3,1-4 and assuming $\phi = 150$ deg.

$$\begin{aligned} AR &= 2 \tan(\phi/2) \sin \beta' \\ &= 7.46 \sin \beta' \end{aligned} \quad (1-12)$$

Using equation 1-3, 1-4, 1-10 the equation be,

$$H_{nom} = \left(\frac{F_n}{P_0 AR^{1+ex}} \right)^{\frac{1}{2+2 \cdot ex}} \quad (1-13)$$

$$W_{nom} = \left(\frac{F_n}{P_0 AR^{1+ex}} \right)^{\frac{1}{2+2 \cdot ex}} \cdot AR \quad (1-14)$$

Then to be conservative taking the ice spalling effect into account the load area described in equation 9 has been reduced, but the force will be same and pressure will rise. So the dimension of design load patch,

$$w = W_{nom}^{wex} = W_{nom}^{0.7} = F_n^{0.389} P_0^{-0.389} AR^{0.35} \quad (1-15)$$

$$b = \frac{w}{AR} = F_n^{0.389} P_0^{-0.389} AR^{-0.65} \quad (1-16)$$

In equation 12, frame angle β' should not be less than 10 degree so that AR will be minimum 1.3 in bow region and for non-other than bow AR is fixed 3.6. [1]

Then the line load and pressure can be obtained as below:

$$Q = \frac{F_n}{w} = F_n^{0.61} \frac{CF_D}{AR^{0.35}} \quad (1-17)$$

$$P = \frac{Q}{b} = F_n^{0.22} CF_D^2 AR^{0.3} \quad (1-18)$$

The maximum value of F, Q and P occurs in different location of bow. So for determining the peak values of F, Q and P, calculation is done at many points at bow with an increment of at least L/20 or minimum 5 points. From every set the largest value of each parameter has chosen to be conservative. Finally largest value set is chosen for obtaining a single design load patch.

1.6. Peak Pressure Factor (PPF)

Having a complex structure of ice in real, the ice loads are quite peaked within the load patch. So, a set of peak pressure factors are used in design formula. The average pressure can be formulated within design load patch

$$P_{avg} = \frac{F}{b \cdot w} \text{ [MPa]} \quad (1-19)$$

Within a higher area, concentrated pressure is more common in load patch and for smaller area; pressure will be higher for local. So to account the concentrated pressure for big area and localized pressure for smaller area PPF is used. PPF is illustrated below,

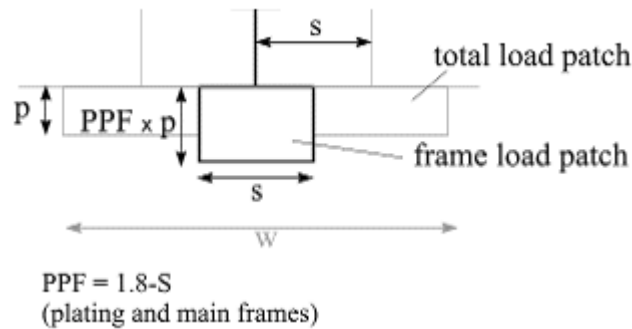


Figure 1-12: Peak Pressure Factor to design individual elements [3]

As the formula given in IACS polar class framing requirements, the following facts are important by giving PPF some minimum value for different framing system.

- For plating member, stiffener spacing is limited to 600mm for transversely framed and 583mm for longitudinally framed structure.
- For stringers, web frames PPF value is 1 if the web frame spacing is half of the ice load patch width.

So after the total description of ice load derivation, design loads are developed in several stages.

Firstly, the total load is minimum than the crushing and flexural limiting load for the design ice.

Secondly, the load patch is idealized.

Thirdly, load distribution within the idealized load patch is modified to account for local loading peaks.

1.7. IACS Structural Requirements

A polar class ship has to face random ice loading with a possibility of extreme load magnitude. To satisfy this demand, when designing a polar class ship, possibility of overloading must be considered. The IACS Unified Requirements has followed simplified plastic collapse mechanisms as design criteria for the structural members. It is called simplified because it is assumed the material is perfectly plastic and the collapse mechanism contains shear-bending moment hinge that means membrane and strain hardening effects are neglected but in real both of these are so obvious.

1.7.1. Membrane effect

In ship hull construction, plate fittings are continuous and the plate gets membrane force from adjacent plates. When we consider membrane effect, the capacity of a plate increases with respect to lateral deflection, as shown in Figure 1-13. Even when a member get enough lateral support, for plate support is from adjacent plate, shear failure not be critical (Amdhal, 2004) [8]. Daley has shown his derivation regarding the IACS UR neglecting the membrane effect. So Daley's derivation should give lower value than the real.

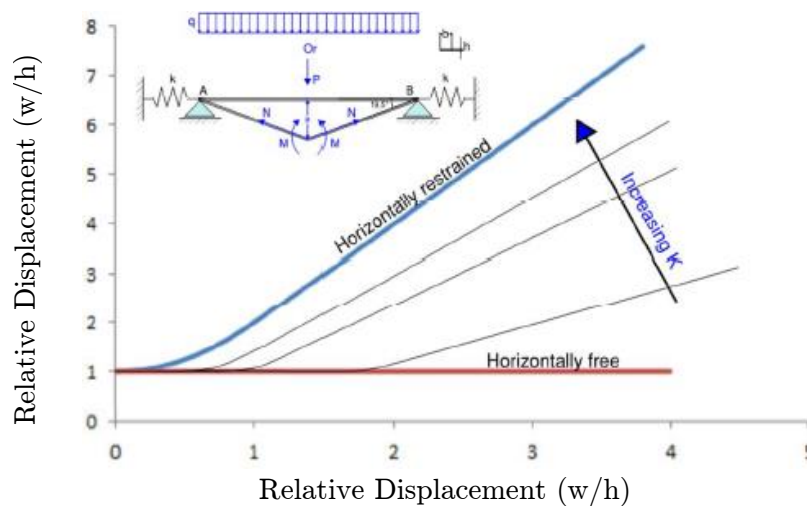


Figure 1-13: Load-deflection curves including membrane effect [9] [10]

1.7.2. Energy Method

In IACS unified requirement the derivation of plastic framing requirements for polar ships is based on the shear plastic collapse mechanisms using work-energy principles [11].

Before applying energy method, right response mechanism (collapse mechanism) has to be chosen which has minimum capacity [9] [2], as this will be closest to the capacity that the structure actually provides. Even then choosing the minimum this is the upper bound to capacity. The chosen mechanism is valid for the regarding boundary condition and the material is assumed ideally plastic.

1.7.3. Collapse Mechanism

To understand the collapse mechanism, as explained by Tore H. Soreide [9] and Amdhal [2], the plastic mechanism for a clamped frame subjected to a uniform load develops through the following step:

First step: Increasing the load q steadily from zero upto yield occurs. This yield load is denoted as q_y and the elastic moment M_y . So the bending moment at this stage,

$$M_y = \frac{q_y l^2}{12} \quad (1-20)$$

Second step: Then load increase until q_1 , so that ends reach maximum moment M_p i.e. be fully plastic and plastic hinge form at two ends.

$$M_p = \frac{q_1 l^2}{12} \quad (1-21)$$

And moment at middle which is not plastic yet,

$$M_{p1} = \frac{q_1 l^2}{24} \quad (1-22)$$

Third step: After reaching the maximum moment at end, it cannot take any moment more. So beam act as simply supported beam. In this condition, further load q_2 applied upto reach maximum moment M_{p2} and the beam center turns into 3rd plastic hinge. So the moment, considering as simply supported at middle,

$$M_{p2} = \frac{q_2 l^2}{8} \quad (1-23)$$

So total moment at middle of the beam,

$$M_p = M_{p1} + M_{p2} = \frac{q_1 l^2}{24} + \frac{q_2 l^2}{8} \quad (1-24)$$

Combining equation 1-21, and 1-24,

$$M_p = \frac{q_2 l^2}{4} \quad (1-25)$$

Now, the total load so far to form 3 plastic hinge is,

$$q_c = q_1 + q_2 \quad (1-26)$$

Combining equation, 1-22, 1-25 and 1-26, we get the collapse load,

$$q_c = 16 \frac{M_p}{l^2} \quad (1-27)$$

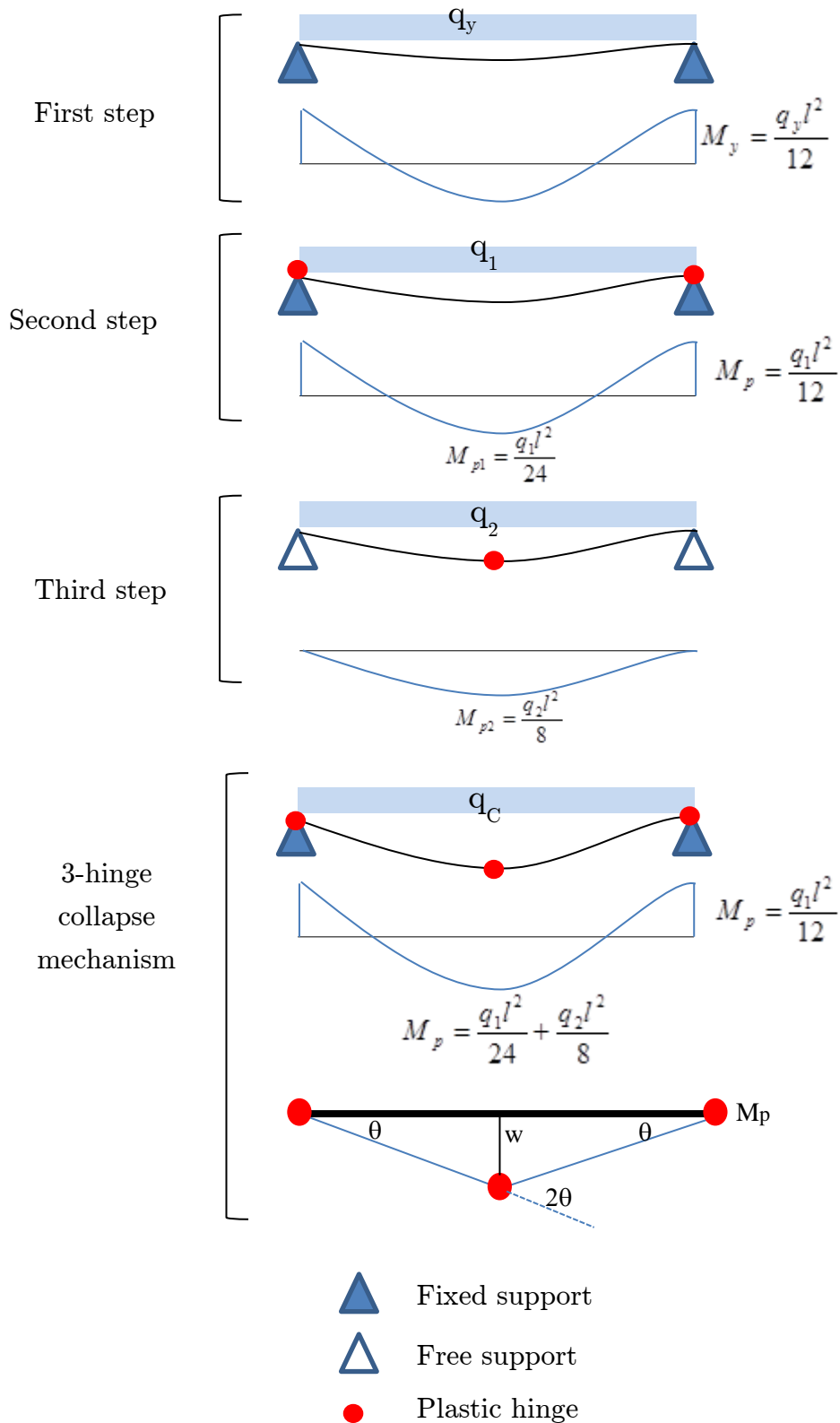


Figure 1-14: Formation of 3-hinge collapse mechanism for uniformly loaded beam

Load development and material behavior during formation of 3-hinge in Figure 1-14 is shown below:

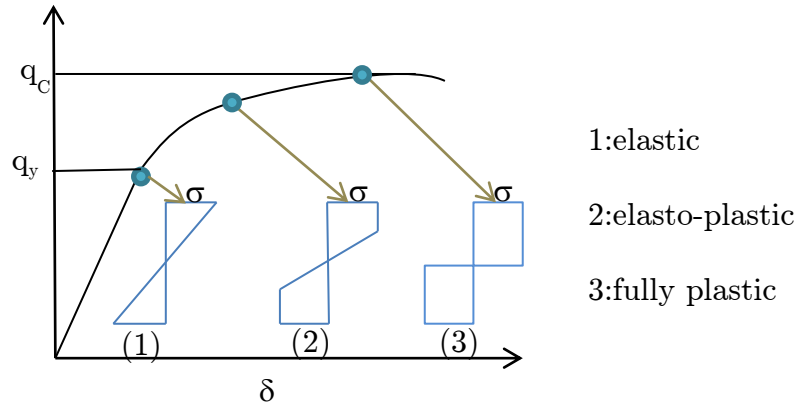


Figure 1-15: load development and material behavior during formation of 3-hinge

1.7.4. Moment and shear interaction

Daley has derived the framing requirements for IACS considering shear interaction i.e. shear stress in web section. When shear capacity increase then plastic moment capacity will decrease. Shear-moment interaction has been showed below:

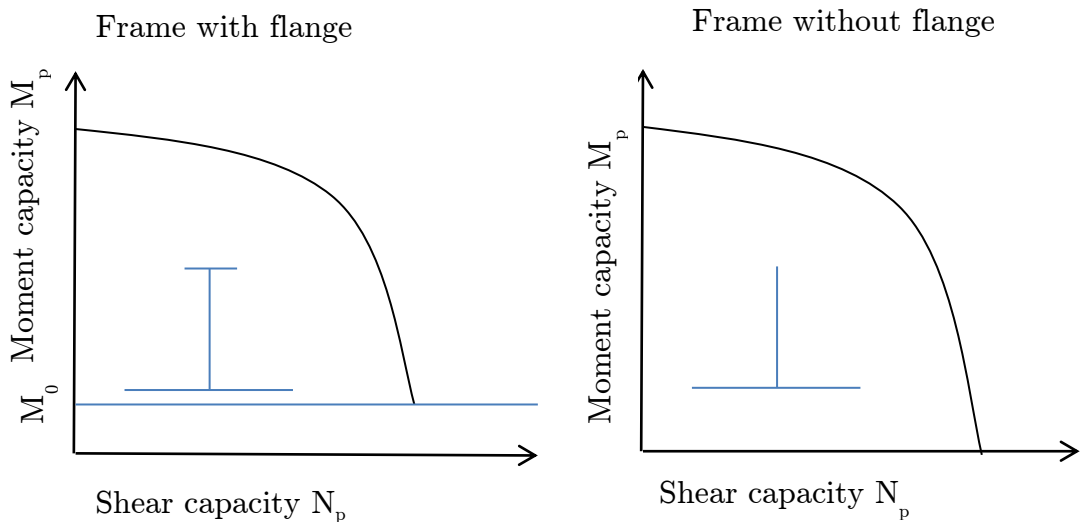


Figure 1-16: Shear-Moment interaction [11]

Normally it is assumed that shear totally carried by the web. So for a flanged

frame, if web be fully plastic in shear even then frame will have the moment capacity as M_0 . So practically frame has been designed in that way so that it could work in a combined way with significant moment and shear capacity. So at the ends reduced moment capacity, M_{pr} has been used in Daley's derivation. Shear-moment interaction can be expressed in following way [4]:

$$\left(\frac{M}{M_{ult}}\right)^2 + \left(\frac{T}{\alpha T_{ult}}\right)^2 = 1 \quad (1-28)$$

Where,

α =Section dependent, greater than or equal to one

M= Bending moment

T= shear capacity

1.7.5. Collapse mechanisms in IACS requirements

In the IACS Unified Requirements rules for framing requirements are based on energy principles so that the external energy is equal to internal energy. The following assumptions has taken into account,

- Rigid plastic material behavior
- Ignores large deformation effects: membrane, strain hardening etc.

IACS has considered the following energy absorbing mechanisms, where the energy is assumed to be dissipated at the hinges.

1. Pure bending hinge

Considering a centrally patch loaded frame. Boundary condition of ends could be fixed-fixed or fixed-simply supported.

2. Combination of shear and bending hinge

When we consider a both clamped ends. In the fixed boundary condition shear force develop. Due to having shear stresses the plastic capacity will be reduced to M_{pr} .

3. Shear hinge

This hinge form when considering an asymmetrical patch load. The both ends can transfer the moment to the adjacent structure. Boundary condition is considered as fixed-fixed.

1.7.6. Centrally loaded patch

Cross sectional area of the attached plate normally be larger than the local frame so that it is assumed that plastic neutral axis is at the intersection point of the frame and the plate [11], shown in Figure 1-17.

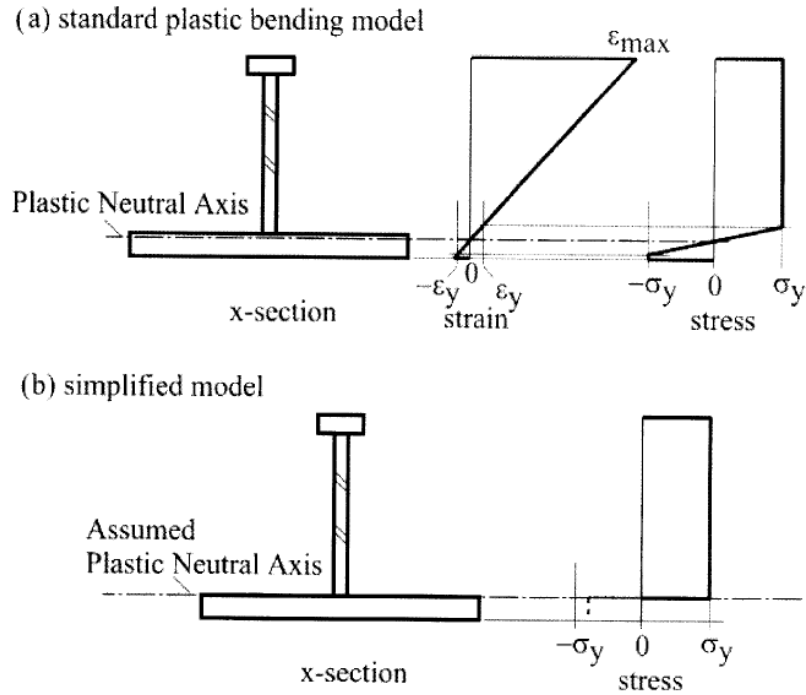


Figure 1-17: Simplified Plastic Modulus concept [11]

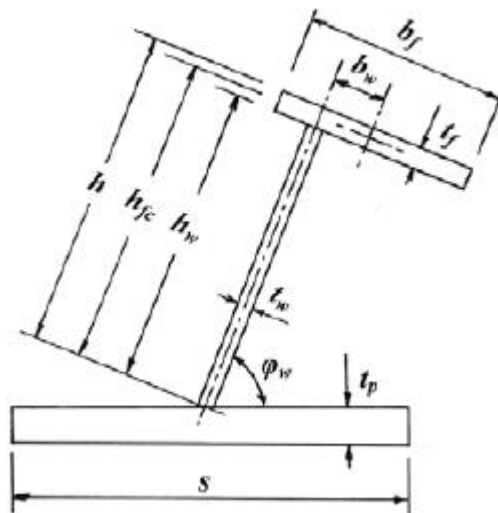


Figure 1-18: Cross section dimensions as defined by IACS [1]

So that the plastic section modulus is,

$$Z_p = A_f \left(\frac{t_f}{2} + h_w + \frac{t_p}{2} \right) + A_w \left(\frac{h_w}{2} + \frac{t_p}{2} \right) \quad (1-29)$$

If the neutral axis situated above the intersection point and it is assumed the angle $\phi_w=90$ then the neutral axis,

$$Z_{na} = \frac{A_f + h_w t_w - t_p s}{2t_w} \quad (1-30)$$

And the exact plastic section modulus will be,

$$Z_{p,exact} = t_p s \left(Z_{na} + \frac{t_p}{2} \right) + \frac{((h_w - Z_{na})^2 + Z_{na}^2) t_w}{2} + A_f (h_{fc} - Z_{na}) \quad (1-31)$$

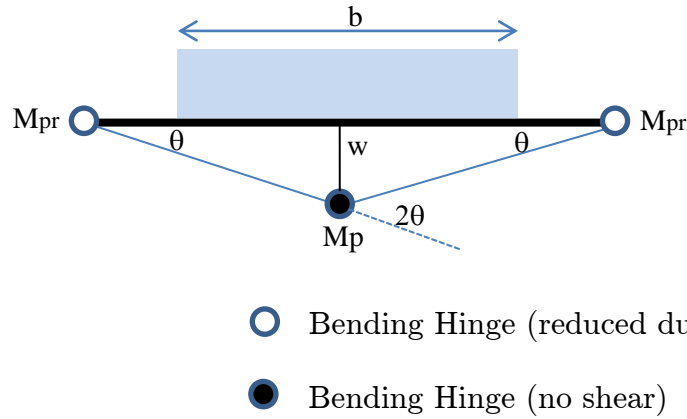


Figure 1-19: 3-hinge Collapse Mechanism for centrally patch loaded frame with fixed-fixed ends

Now, applying energy method for frame in Figure 1-19,

$$\begin{aligned}
 W_e &= \int_{-b/2}^{b/2} P.S.w(x)dx \\
 &= 2 \int_0^{b/2} P.S.w(x)dx \\
 \text{External work,} \quad &= 2P.S.\delta \int_0^{b/2} \left(1 - \frac{2}{L}x \right) dx \\
 &= P.b.S.\delta \left(1 - \frac{b}{2L} \right)
 \end{aligned} \quad (1-32)$$

Internal work,

$$W_i = \delta \left(\frac{4M_p}{L} + \frac{4M_{pr}}{L} \right) \quad (1-33)$$

So, equating external and internal work we get,

$$P.b.s. \left(1 - \frac{b}{2L} \right) = \left(\frac{4M_p}{L} + \frac{4M_{pr}}{L} \right) \quad (1-34)$$

If we don't consider reduced plastic moment, then we get the capacity equation as follows,

$$P = \frac{8M_p}{L.b.s. \left(1 - \frac{b}{2L} \right)} \quad (1-35)$$

Where,

P = the patch pressure

S = frame spacing

$M_p = Z_p \sigma_y$

$M_{pr} = Z_{pr} \sigma_y$

σ_y = yield stress

As derived by Daley [11] reduced section modulus,

$$Z_{pr} = Z_p \left(1 - k_w \left(1 - \sqrt{1 - \left(\frac{A_0}{A_w} \right)^2} \right) \right) \quad (1-36)$$

Where, minimum shear area, $A_0 = \frac{1}{2} P b S \frac{\sqrt{3}}{\sigma_y}$ (1-37)

$$k_w = \frac{Z_w}{Z_p} \quad (1-38)$$

When web will be fully effective in bending, Z_{pr} will be equal to Z_p . So using equation 1-34, minimum section modulus,



$$Z_0 = \frac{PbS}{8\sigma_y} \left(1 - \frac{b}{2L}\right)L \quad (1-39)$$

So finally we get the capacity for 3-hinge collapse by using equation 1-34, 1-36, 1-37, 1-38

$$P_{3h} = \frac{(2-k_w) + k_w \sqrt{1 - 48Z_{pns}(1-k_w)}}{12Z_{pns}k_w^2 + 1} \frac{4Z_p\sigma_y}{[SbL(1-b/2L)]} \quad (1-40)$$

Where,

$$Z_{pns} = \left[\frac{Z_p}{A_w L \left(1 - \frac{b}{2L}\right)} \right]^2 \quad (1-41)$$

For the term under the root sign of equation (40) to stay positive, Z_p must be less than Z_{pmax} ,

$$\text{Where, } Z_{p,max} = \sqrt{\frac{1}{48(1-k_w)} A_w L \left(1 - \frac{b}{2L}\right)} \quad (1-42)$$

When Z_p will be greater than Z_{pmax} then shear failure will occur at frame first and the capacity will be limited to,

$$P_{lim} = \frac{2}{\sqrt{3}} \frac{A_w \sigma_y}{Sb} \quad (1-43)$$

1.7.7. End load case (Asymmetric load)

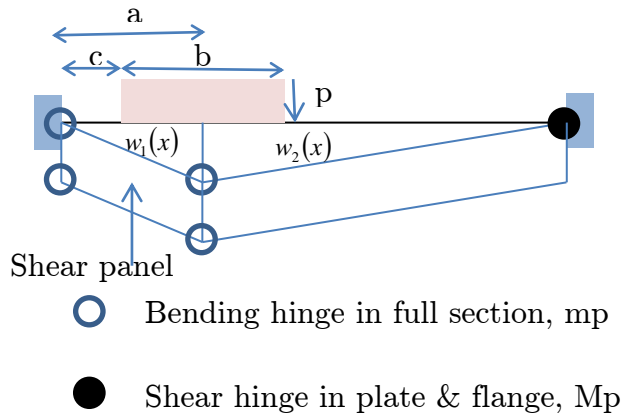


Figure 1-20: End loaded fixed-fixed frame, with assumed plastic mechanism

From the Figure 1-20 the external work is found by integrating the external load over the deformation. So the external work is,

$$\begin{aligned}
 W_e &= \int_c^{c+b} P.S.[w(x)].dx \\
 &= PS \left[\int_c^a \frac{x}{a} dx + \int_a^{c+b} \left(1 + \frac{x-a}{a-L} \right) dx \right] \quad (1-44) \\
 &= PS \left[\frac{(a+c)(a-c)}{2a} + \frac{b+c-a}{L-a} \left(L - \frac{a+b+c}{2} \right) \right]
 \end{aligned}$$

Find the location of c which will give the maximum external work.

$$\frac{d}{dc} W_e = 0 \quad (1-45)$$

This gives, $c = a \left(1 - \frac{b}{L} \right)$ (1-46)

Using equation, 1-44, 1-46 we get the maximum external work for asymmetric loading condition,

$$W_{e,asym} = PbS \left(1 - \frac{b}{L} \right) \quad (1-47)$$

For internal work, taking 4-shear hinges in shear panel and one bending hinges in the other end, the internal work for unit deflection will be,



$$W_i = N + M_p \frac{1}{L-a} + m_p \left(\frac{2}{a} - \frac{1}{L-a} \right) \quad (1-48)$$

Then equating the external and internal work and after some calculation (details in paper of Daley [11]) the shear capacity for this condition can be given by,

$$P_s = \frac{\sigma_y}{bS(1-b/2L)} \left[\frac{A_w}{\sqrt{3}} + \frac{Z_p}{L} (1.1 + 5.75k_z^{0.7}) \right] \quad (1-49)$$

2. Comparison of Polar Classes

IACS UR is classified into 7 polar classes PC1 to PC7. Among these polar classes the PC1 is the heaviest class with respect to strength which permits the structure to trade in year round ice condition and PC7 is the lightest. The requirements vary among these seven polar classes from many aspect of view. Comparison, differences, the different way of implementation of the requirement and the important parameters among these polar classes; all are discussed below:

2.1. Ice load

- For all polar class a glancing scenario on the bow area is considered as the design scenario.
- The parameters to define the ice load are
 - Average pressure(P_{avg})
 - Design load patch width(w) and breadth(b)
 - Total glancing impact force(F)
 - Line load(Q)
 - Shape co-efficient(f_a)
- The above mentioned parameters has to be calculated for the specific hull area as a **function of bow shape** for regarding polar class as shown below:

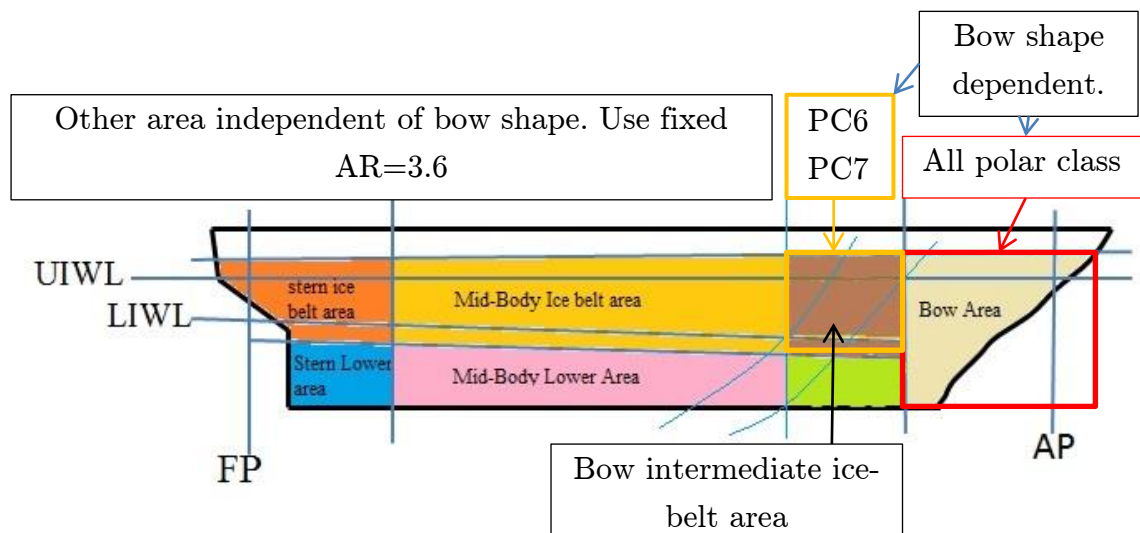


Figure 2-1: Ice load parameter dependency on hull area

- Class dependent parameters define the glancing impact nature. Class factors are formulated as given discussed in earlier chapter.
 - Crushing class factor: $CF_C = P_0^{0.36} V_{ship}^{1.28}$
 - Flexural class factor: $CF_F = \sigma_f h_{ice}^2$
 - Patch class factor: $CF_D = P_0^{0.389}$

These formulas are showing that, ship speed, ice flexural strength, nominal ice thickness all are constant class dependent. The values are given below:

Table 2: Class factors [1]

Polar Class	Crushing Failure Class Factor (CF_C)	Flexural Failure Class Factor (CF_F)	Load Patch Dimensions Class Factor (CF_D)	Displacement Class Factor (CF_{DIS})	Longitudinal Strength Class Factor (CF_L)
PC1	17,69	68,6	2,01	250	7,46
PC2	9,89	46,8	1,75	210	5,46
PC3	6,06	21,17	1,53	180	4,17
PC4	4,5	13,48	1,42	130	3,15
PC5	3,1	9	1,31	70	2,5
PC6	2,4	5,49	1,17	40	2,37
PC7	1,8	4,06	1,11	22	1,81

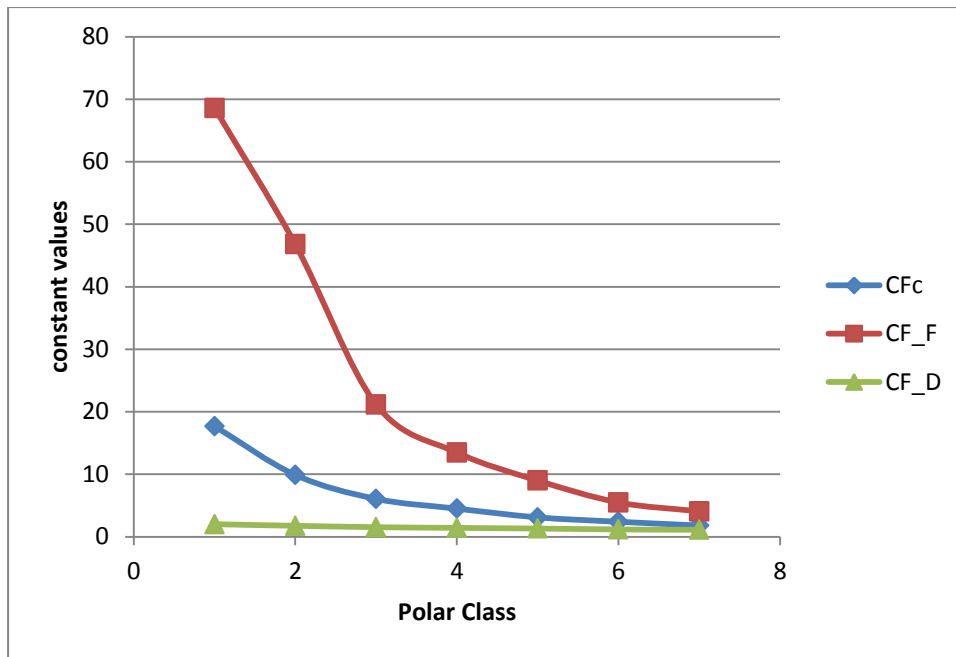


Figure 2-2: Class factor variations

As it is seen from above figure, flexural class factor values varies so much compared to crushing factor. The dimension load patch factor is almost so close for all polar class. For better understanding let recall the force equation 1-9 and shape coefficient fa again,

$$F_n = fa \cdot CF_C \cdot \Delta_{ship}^{0.64}$$

For higher polar class, flexural factor is so much high which permit crushing force to a substantial limit. That means the structure of higher polar class has been given better crushing ability. But the load patch dimension factor doesn't change as the load changing. So that simplified design load patch dimension has been kept approximately close for all polar classes (see Figure 2-4).

- From force equation 1-9, it can be said that the ice force is dependent on ship size and bow angles. So ice force is dependent on ship shape i.e. ship's displacement. Pressure and load dimension variance for different displacement has been shown below. The calculations have been done for 'mid-body ice belt area'.

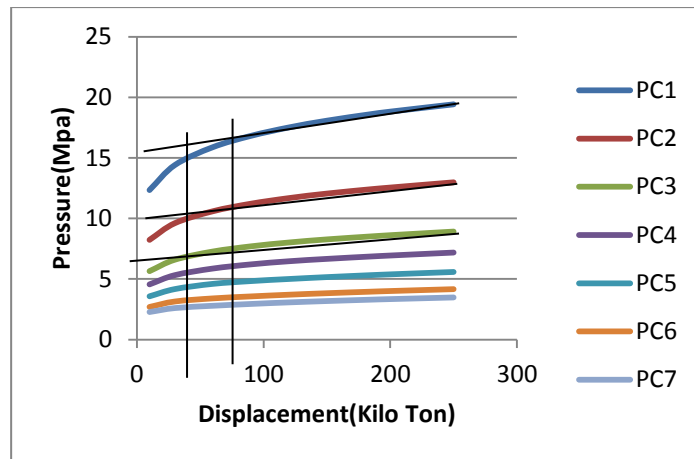


Figure 2-3: Pressure variance for different displacement

From above figure it can be said that ice load is obtained much higher for PC1 & PC2 compared to other class. And pressure variance is also higher for PC1 and PC2. Pressure variance is linear when displacement is more than 90 Kilo Ton for PC1 and PC2. For PC3-PC7 pressure variance is linear when ship displacement is more than 60 Kilo Ton.

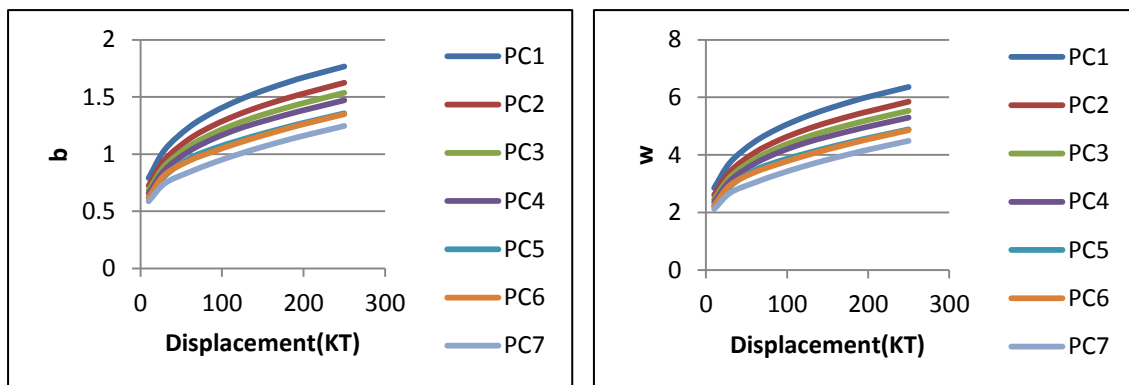


Figure 2-4: Load Patch dimension variations

From the above two curves set, variation of dimensions is quite regular compared to the pressure variation. For a displacement, like 250 KT, where pressure is varying from 3 MPa to 19 MPa but load height is changing from 1.2 m to 1.8 m and width 4.4m to 6.3m only. As load area is not increasing as pressure increase, higher polar class is intended to face more local pressure than lower polar class. So local strengthening will be a requirement for higher polar class.

2.2. Framing Requirements

2.2.1. Shell plate requirements

As given in IACS req. 2011, the shell plate thickness (unit: mm) is

$$\text{For transversely framed plating, } t_{net} = 500s \left(\frac{AF \cdot PPF_p \cdot P_{avg}}{\sigma_y} \right)^{0.5} \frac{1}{1 + \frac{s}{2b}} \quad (2-1)$$

$$\text{For longitudinally framed, when } b \geq s; t_{net} = 500s \left(\frac{AF \cdot PPF_p \cdot P_{avg}}{\sigma_y} \right)^{0.5} \frac{1}{1 + \frac{s}{2l}} \quad (2-2)$$

$$\text{when } b < s; t_{net} = 500s \left(\frac{AF \cdot PPF_p \cdot P_{avg}}{\sigma_y} \right)^{0.5} \left(\frac{2b}{s} - \left(\frac{b}{s} \right)^2 \right)^{0.5} \frac{1}{1 + \frac{s}{2l}} \quad (2-3)$$

Where,

s = transverse frame spacing in transversely-framed ships or longitudinal frame spacing in longitudinally-framed ships [m]

AF = Hull Area Factor

PPF_p = Peak Pressure Factor

P_{avg} = average patch pressure [MPa]

σ_y = minimum upper yield stress of the material [N/mm²]

b = height of design load patch [m]

l = distance between frame supports[m].

From the above equations, plate thickness is dependent on pressure which means dependent on ship displacement, and the frame arrangements.

For a specific framing arrangement, the plate thickness variation is proportional to $P^{0.5}$. So the variations show the same trend as pressure variations as shown in Figure 2-5. These thicknesses are for frame spacing 600mm and span length 2.215 m for a longitudinally framed FPSO.

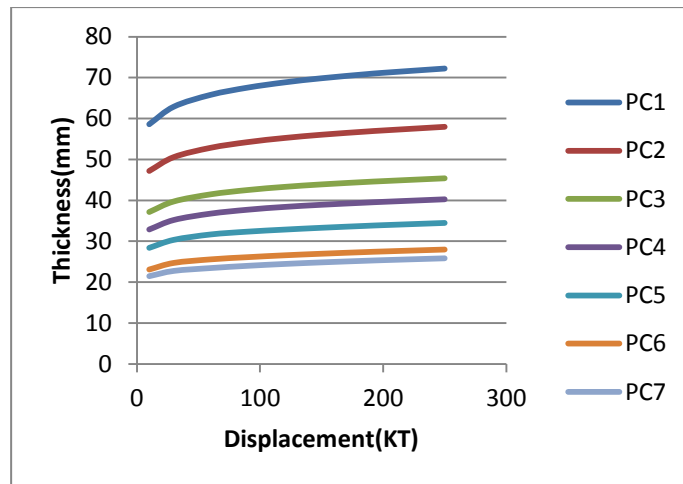


Figure 2-5: Thickness variations

For a specific displacement thickness requirements change linearly with frame spacing. IACS rules limit the frame spacing to maximum 600 mm for plating members considering the peak pressure factor discussed earlier. From Figure 2-5 & Figure 2-6, plating thickness is much higher for PC and PC2 comparing to others as it was discussed earlier that for higher polar class local high pressure is much higher.

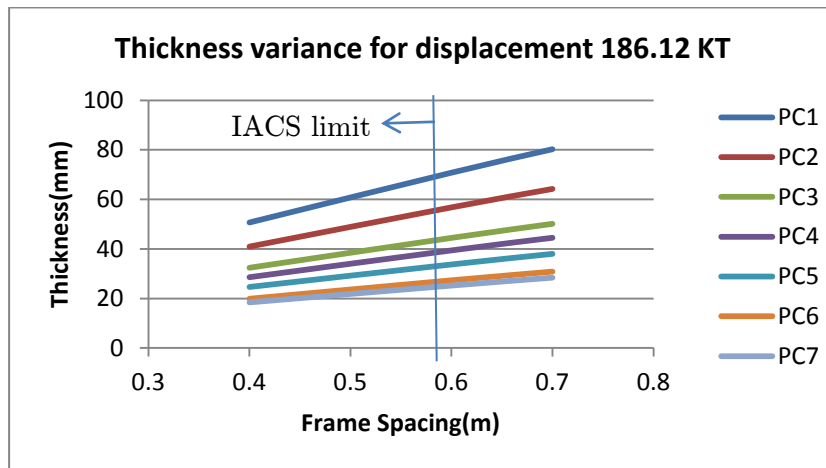


Figure 2-6: Thickness variation as frame spacing changes

2.2.2. Shear Area

Minimum shear area (equation 1-37) is modified in IACS req. 2011 [1] as given as below; for longitudinally ships,

$$A_L = \frac{100^2 \cdot AF \cdot PPF_s \cdot P_{avg} \cdot 0.5 \cdot b_1 \cdot a}{0.577 \cdot \sigma_y} \text{ [cm}^2\text{]} \quad (2-4)$$

Where,

PPFs = Peak Pressure Factor

$b_1 = k_o \cdot b_2$ [m]

$k_o = 1 - 0.3 / b'$

$b' = b / s$

$b_2 = b \cdot (1 - 0.25 \cdot b')$ [m], if $b' < 2$

$= s$ [m], if $b' \geq 2$

$a =$ longitudinal design span [m]

Calculating the minimum shear area required for frame spacing of 600mm, span length of 2.215 m and ship displacement 186.12 KT

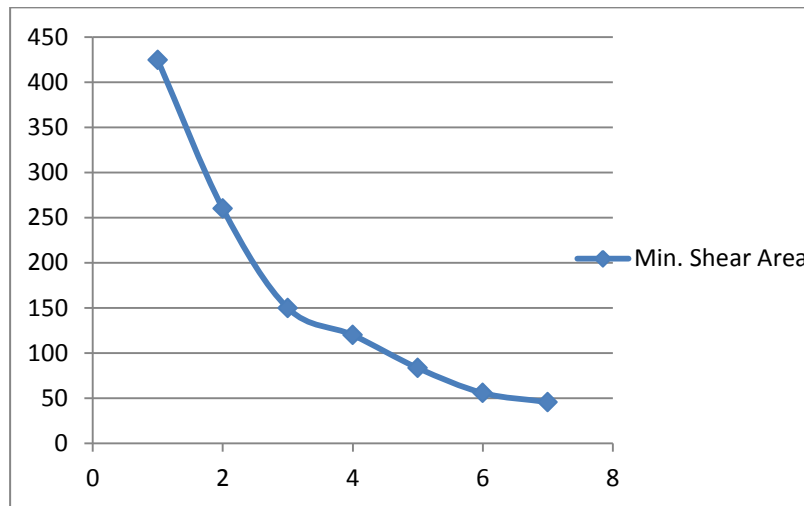


Figure 2-7: Min shear area requirements as IACS

From above figure, there is a huge difference between lightest and heaviest polar class. For polar class PC1 and PC2 need heavy longitudinal frame to protect shear failure which could be achieved by giving higher web height.

3. IACS UR for a moored Arctic FPSO

The failure modes of an ice sheet are mainly compression failure i.e. crushing and flexure failure i.e. buckling, bending etc. For trading in polar waters, the main challenge is to crush or bend the ice while the ship moves. The structure must have the strength to resist the ice bending force. But for a moored FPSO, it is different. The force is from drifting ice and it bends itself to the FPSO. So a moored FPSO has to be strength enough to resist the drifting ice pressure.

The normal ice load is expressed as equation (1-9)

$$F_n = fa \cdot CF_C \cdot \Delta_{ship}^{0.64}$$

For a moored FPSO, the vessel velocity which is class dependent is not related to this case. The other factors such as the ice thickness, strength of ice data for a polar class are predetermined. These data can be found from the environmental data for a specific area. So as discussed earlier, the main parameter that can be changed is hull shape or more specifically bow shape.

Another challenge is to keep the FPSO face to the opposite of the ice drift (Figure 3-1). In addition the ice drift direction changes always because of wind and current. So the designing of an effective mooring system is necessary and make it sure that its ice vaning capacity is at its best. Ice vaning is the capability of the FPSO to keep the bow direction always towards to drift direction.



Figure 3-1: Ice vaning: Ice drifts and ship direction [12]

A moored ship scenario is quite different than a moving one. For a moving FPSO, in the energy balancing equation (1), normal kinetic energy includes the mass of ship but in this case it will be drifting ice sheet mass. So the kinetic energy equation will be for ice sheet. The mooring system and FPSO itself has to be strength enough to resist the kinetic energy of ice sheet. The wedge based (Figure 1-5) collision which determines the nominal contact area, $A = \frac{WH}{2}$ should also be different for moored condition which will make the ice load calculation different.

4. Assessment of a FPSO

Floating production, storage and offloading (FPSO) unit is familiar in the offshore oil and gas industry. This thesis work was motivated by a FPSO named 'white Rose Field Husky Oil FPSO' which was built under DNV class. She had been built to operate in White Rose oil field, 350km off the coast of Newfoundland and operated by Husky Energy; build by Samsung heavy industries co. ltd. [13].

This FPSO was interesting to choose because DNV class framing requirements calculation method is different to IACS. So by assessing this FPSO, we will get a comparative assessment with IACS requirements.

In this thesis work I worked with a larger part of the ship side. As IACS hull area definition (Figure 1-2), the main focus is on mid-body ice belt area.

Principle particulars are given in below table (source-provided by supervisor):

Table 3: Principle particulars of the FPSO

Ship length O.A.	267 m
Length LBP	258 m
Breadth	46 m
Depth	18.60 m
Block coefficient(assumed)	0.85
Displacement	186.12 KT
Frame Spacing	600 mm

Now this side structure contains (Figure 6-1) side plating, longitudinal frames, normal web frame, heavy web frame, heavy stringers and stiffeners attached to web and stringer. The dimensions and material properties are given below:

Table 4: Side Structure Dimension details

Component	Dimension/Thickness(mm)	Material Property(Yield)(MPa)
Side plate	23	315
Side Longitudinal	250x12+75x12	315
Ordinary web	850x15	250
Ordinary web stiffener	200x15	250
Stringer	2200x14(1),13(2)	315
web	2200x13	315
Stiffener'-Web	150x12	250
Stiffener'-stringer	200x12	250

We don't know the exact polar class of this FPSO. So that as in IACS, all the calculations will be done for seven polar classes which include the calculation of ice load, framing requirements (Table 5). Using equation 1-15 to 1-18

Table 5: IACS calculated values for 186.12 KT displacements FPSO

Polar class	Avg. Pressure(MPa)	Load Patch dimension		Plate thickness required (mm)	Min. Shear area required (cm ²)
		b(mm)	w(mm)		
PC1	18.62816	1.641016	5.907657	72.22067	424.4423141
PC2	12.42501	1.502393	5.408614	57.96707	259.8937663
PC3	8.527931	1.419833	5.1114	45.3787	149.7410758
PC4	6.868485	1.358058	4.889009	40.24341	119.8065597
PC5	5.326514	1.248378	4.49416	34.46314	83.3298355
PC6	3.963362	1.235606	4.448182	27.9617	55.70660705
PC7	3.301475	1.135341	4.087227	25.81568	45.57204206

Existing side plate thickness of this FPSO is 23mm. So it doesn't match with even the lightest polar class of IACS. So, it will be checked later that it can carry the load of 3.3 MPa which is the lowest load calculated for this displacement or not.

- **Shear area calculation**

The longitudinal used in this FPSO are originally bulb profile. Then for simple dimension it's converted to L profile of dimension given in Table 4. Dimension conversion is based on 'Rukki Profiler' standard shipbuilding profiles [14].

Actual shear area of the longitudinal frame is calculated for the web section of the frame considering corrosion factor of 2mm. So the shear area is $250 \times (12-10)/100=25\text{cm}^2$.

As a requirement of IACS, this shear area has to be greater than the shear area shown in Table 5. But it the actual shear area is approximately half of the required if we consider even the lightest polar class.

- **Framing-structural stability**

As stated in the IACS req. 2011, to avoid local buckling in the web frame, the web frame dimension has to satisfy the following limit values,

For flat bar,
$$\frac{h_w}{t_{wn}} \leq \frac{282}{\sigma_y^{0.5}} \quad (4-1)$$

For bulb, tee and angle sections,
$$\frac{h_w}{t_{wn}} \leq \frac{805}{\sigma_y^{0.5}} \quad (4-2)$$

Minimum net web thickness,
$$t_{wn} = 2.63 \times 10^{-3} \cdot c_1 \sqrt{\sigma_y / (5.34 + 4(c_1/c_2)^2)} \quad (4-3)$$

Where,

hw = web height

twn = net web thickness

σ_y = minimum upper yield stress of the material [N/mm²]

$$c1 = hw - 0.8 \cdot h \text{ [mm]}$$

hw = web height of stringer / web frame [mm]

h = height of framing member penetrating the member under consideration (Figure 4-1)

$c2$ = spacing between supporting structure oriented perpendicular to the member under consideration [mm] (see Figure 4-1)

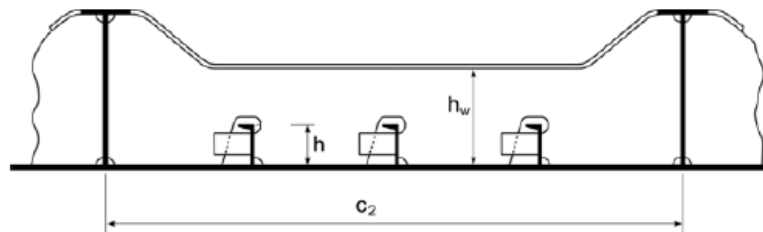


Figure 4-1: Parameter Definition for Web Stiffening [1]

By applying these formulas, it is calculated that the net web thickness requirement is 39mm. Web height to thickness ratio also doesn't satisfy the limit equation for flat bar.

So we will get local buckling on web frame. This will be analyzed later on Abaqus analysis.

5. Non-linear finite element analysis of a single frame

IACS requirements are based on single frame loading. So, single frame analysis should be so precise so that it can represent the entire grillage structure properly. Here a longitudinal frame is intended to analyze analytically and numerically. Within a full span (4.43m) longitudinal, ends are supported with transverse heavy web frame and in middle there is an ordinary web frame (Figure 5-1). Before starting the analysis, it was a question that should we take the full span or half span of 2.23m. If we take, the half span then it would be same as Daley's asymmetric load case (loading description, see chapter 5.5, Figure 5-9). But there is problem with support, because the strength of web frame and ordinary web frame is not equal. Then it was decided to take full span and keep the ordinary frame at middle. So this formation is representing symmetric loading condition. So the analytical model and loading configuration will be based on symmetric loading condition as Daley. From the large part a single longitudinal has been chosen from the ice loaded area as shown figure below:

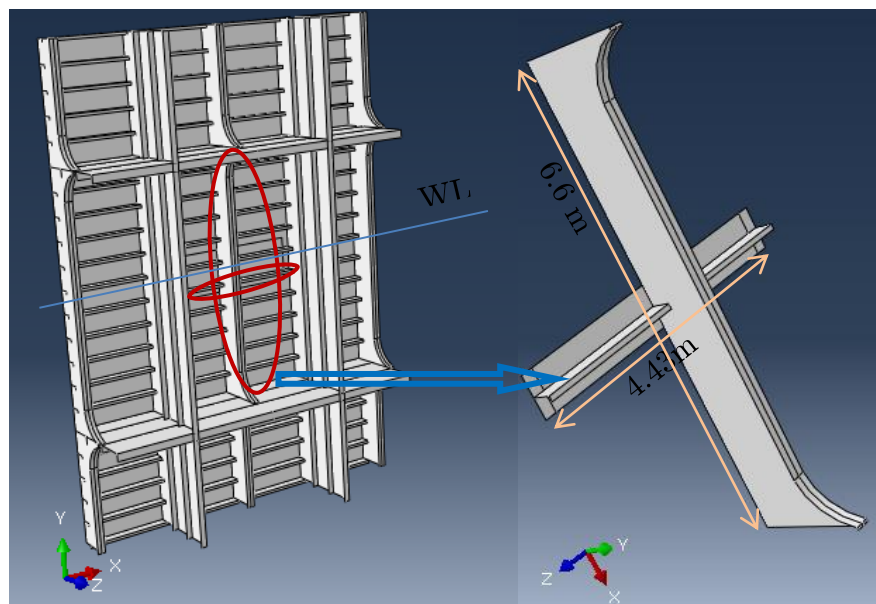


Figure 5-1: Single Frame selection

This longitudinal frame is in mid-body ice belt area (Figure 1-2). Abaqus analysis and analytical formulation procedure are as follows:

5.1. Non-Linear Finite Element Analysis

In linear analysis the displacement is assumed to be small and the material behavior is elastic and linear i.e. follow hooks law. But for realistic analysis and the case like accidental or overloading, non-linearity of geometry and material should consider. A non-linear analysis permits large deformation and consider plastic behavior of material. Then the load-displacement relation differs from linear hooks law stress-strain relation. Non-linear behavior of a typical structure is shown below,

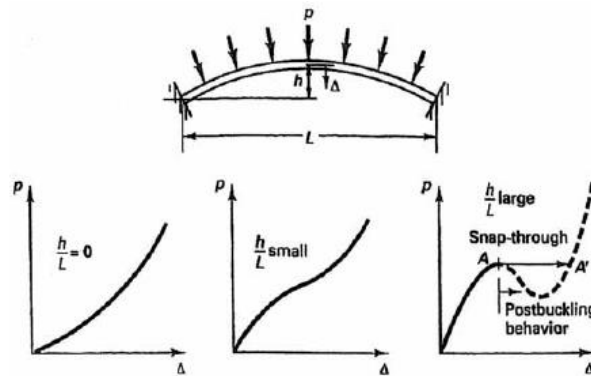


Figure 5-2: Non-linear behavior of a thin plate/shell [15]

For the analysis of ultimate strength or collapse non-linear analysis has to be implemented as it allows large deformation.

Finite element analysis is based 3 principles,

- Equilibrium
- Kinematic compatibility
- Stress-strain relationship

When a structure is allowed for large deformation, unstable behavior of load-displacement curve is frequently observed.

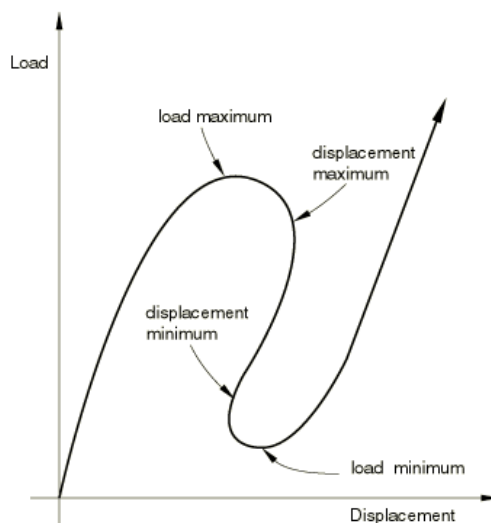


Figure 5-3: Typical unstable response of structure [16]

There are many way to solve this kind of behavior such as arc-length technique. In Abaqus modified Riks method is used to solve such case.

5.2. Finite element model

J. Abraham in his master thesis [17] found that, solid element give higher capacity than shell element so taking shell element will be a conservative selection. Getting idea from this, shell element has been used in my thesis. Abaqus documentation [16] also recommends to use shell element when thickness of the plate, members is significantly lesser than the other dimensions; less than 1/10. Other dimension refers a typical global structural dimension not the element dimensions. Global dimensions are like distance between supports, stiffeners, radius of curvature etc. In Abaqus, it is assumed that the plane perpendicular to the shell mid-surface remain perpendicular after displacement.

5.3. Material Property

Nonlinear model is considered for the structure. The non-linearity is utilized by using the hooks law up to yield stress and then plasticity which permit large deformations. Allowing larger deformations and applying plasticity indicate non-linearity of geometry and material. The following materials property has been taken into account. To relate with IACS rules, in analysis two pure plastic material property has been applied as shown in Figure 5-4 with the standard

steel property; Young Modulus=210,000 MPa and Poison's ration=0.3

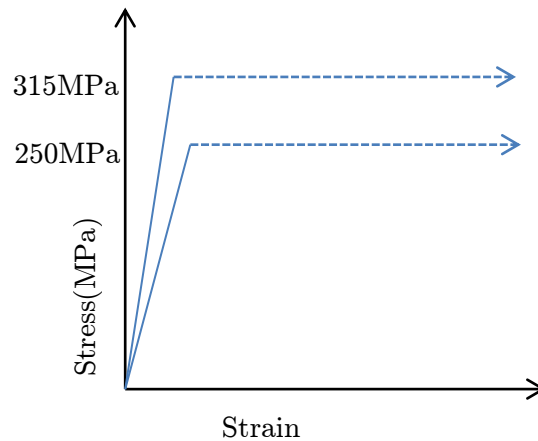


Figure 5-4: Elastic-Purly plastic material behavior

5.4. Boundary Condition

A single longitudinal frame is considered, supported with heavy web frame at the end and one ordinary web frame at the middle (Figure 5-1). The end of the longitudinal is assumed to be welded at the web frame. Before applying the boundary conditions the following facts will be considered:

- Adjacent structure
- Symmetricity
- Supporting structure strength
- Possible translation and rotation ability

Firstly, it was tried to use the following structure to analyze,

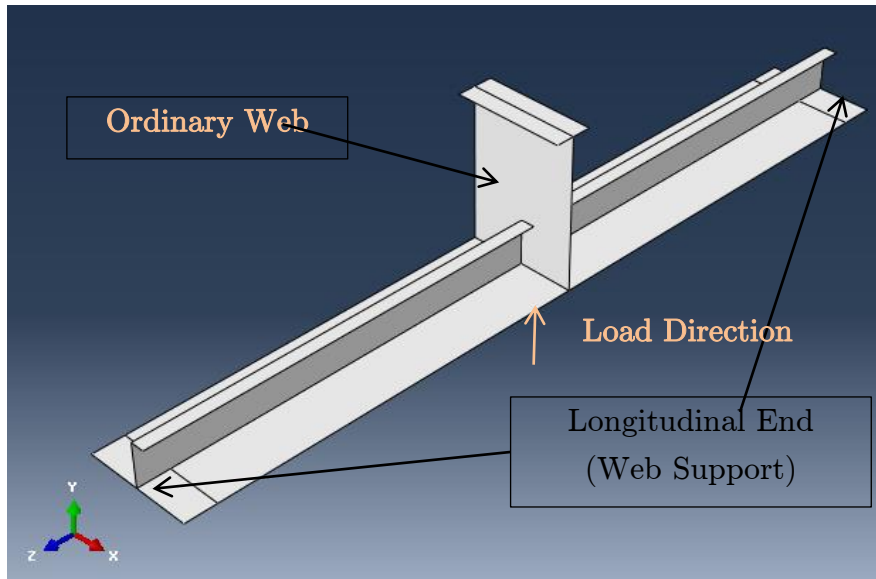


Figure 5-5: Single Longitudinal (First Phase)

It is easy to think, to assume the longitudinal end fixed as having the heavy web support. But it was difficult to set what should be the boundary condition at ordinary web position. This cannot be neither fixed as it is not same strong as the web frame nor free in *y-direction*. If at ordinary web frame position U_y is free, then this frame will not have any effect as the load direction is towards positive *y-direction* (see Appendix, Figure A-4).

Then, it would be a solution to take the full ordinary web length between Longitudinal Stringer as following image

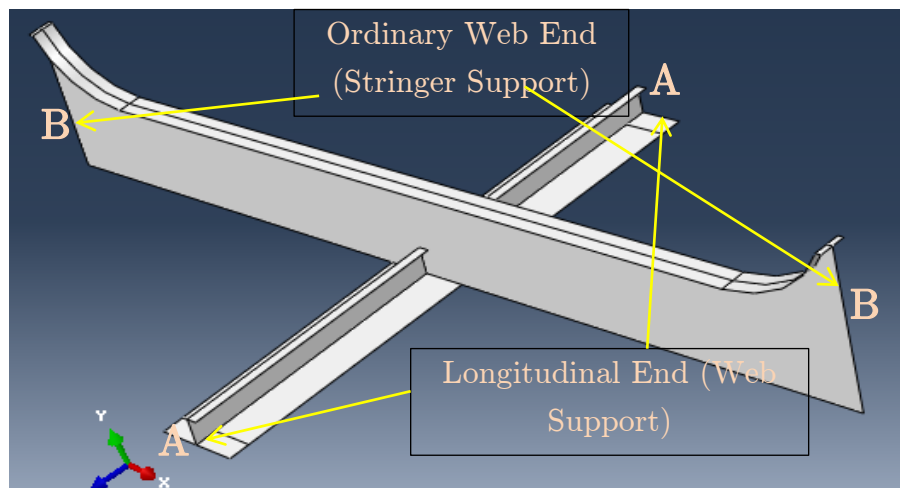


Figure 5-6: Single Longitudinal (Final Phase)

As the A: A end is supported by heavy web frame and B:B end is by stringer end; this ends has been kept **fixed**. The plate is the short part of whole side plating. In the transverse direction(x-direction) both long edge is symmetric. So in x-direction the shell plate has to be restricted to deform due to keep the adjacent plating effect. So this plate edges (red highlighted two edges in Figure 5-7) has been given **symmetric boundary condition**. $U_x=UR_y=UR_z=0$.

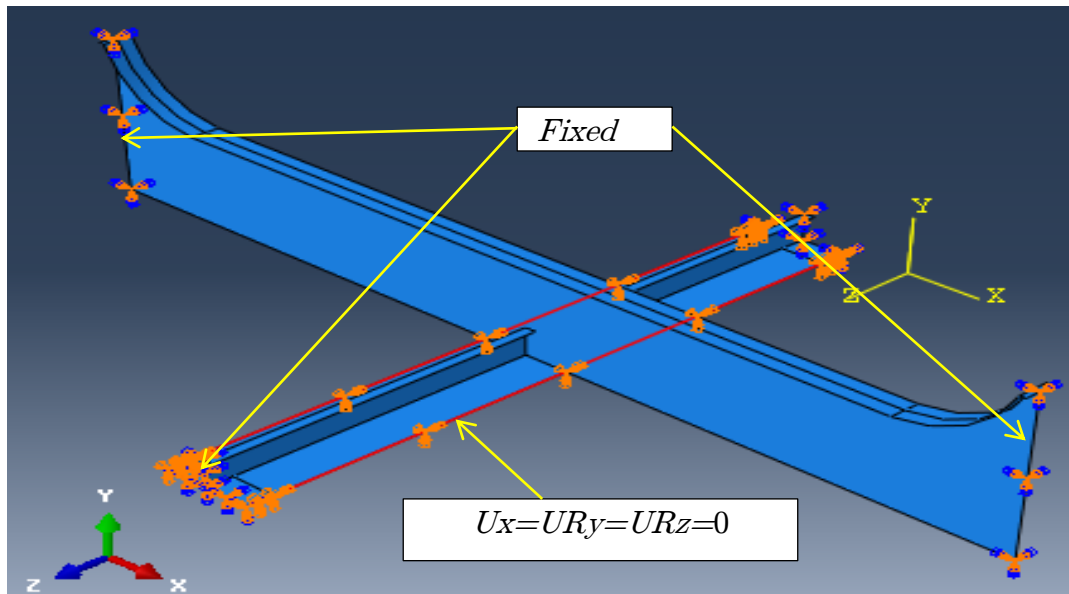


Figure 5-7: Boundary Condition for single Longitudinal Frame

For setting the final boundary condition, the deformation nature in whole grillage part had been observed. From the figure below, longitudinal end (red circled) has been kept fixed analytically, but actually we get deformation in whole grillage analysis.

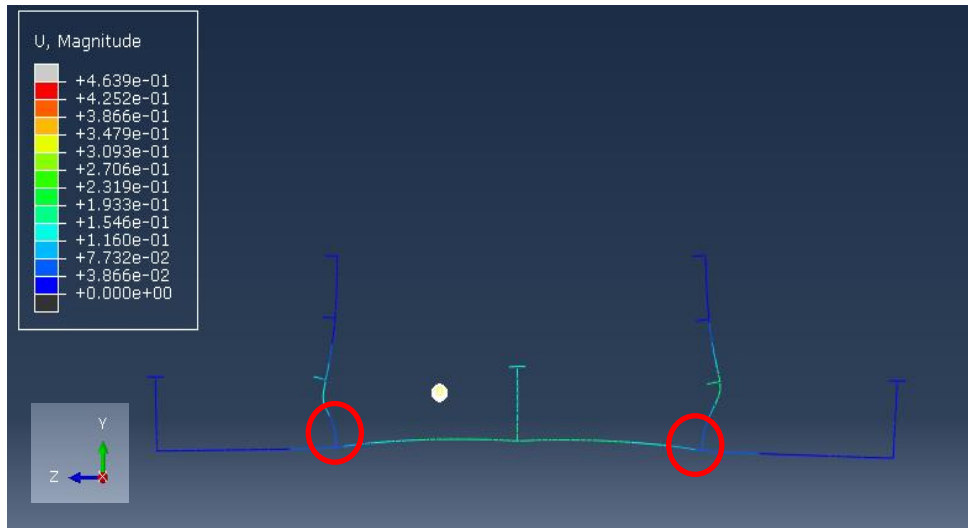


Figure 5-8: Displacement pattern in whole grillage part at 1.5MPa load

5.5. Load

This longitudinal frame is intended to analyze according to IACS PC7 loading configuration. The ice load and the ice load patch dimension are for PC7 as presented in Table 5. Applied pressure 3.3 MPa, Load patch width is 4.08m and the height is 1.13m. So the load is applied over the frame spacing (600mm).

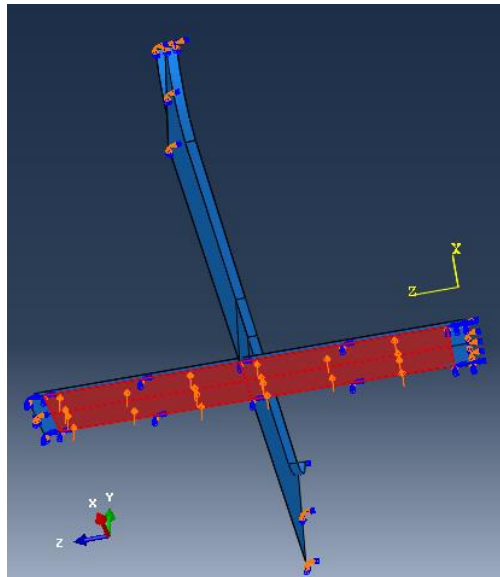


Figure 5-9: Loading of Single longitudinal frame.

5.6. Analytical Formulas

To form a simplified collapse mechanism I have tried different mechanism model. The different models are discussed below:

- 1st Model:

First of all the mechanism is just assumed as the normal 3 hinge model as derived in chapter 1.7.6 that maximum deformation occur at middle for symmetric center load. The addition with that model (Figure 1-19) is a normal web frame has been added of length $1.5L$. (Longitudinal length, $L=4.43\text{m}$ and span length between stringer $6.6\text{m}=1.5L$). Pure bending hinge is assumed where M_L for longitudinal and M_W for Ordinary web frame. Shear reduction is not considered.

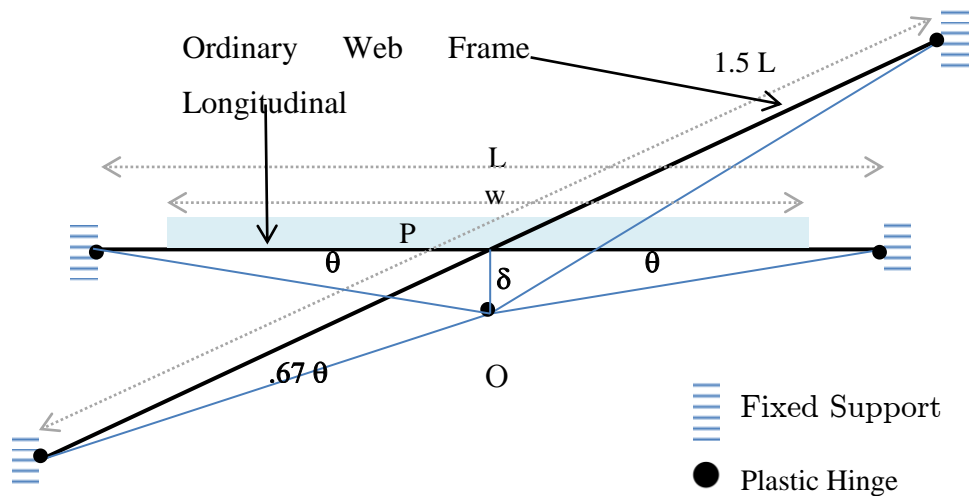


Figure 5-10: Single frame 1st model

External work,

$$W_e = \int_{-w/2}^{w/2} P \cdot s \cdot w(x) dx \quad (5-1)$$

$$= P \cdot w \cdot s \cdot \delta \left(1 - \frac{b}{2L} \right)$$

Internal work,

$$W_i = (4M_L + 2.68M_w) \frac{2\delta}{L} \quad (5-2)$$

Equating 5-1, 5-2 we get the capacity,

$$P_1 = \frac{8M_L + 5.37M_w}{LwS \left(1 - \frac{w}{2L}\right)} \quad (5-3)$$

- 2nd Collapse Model

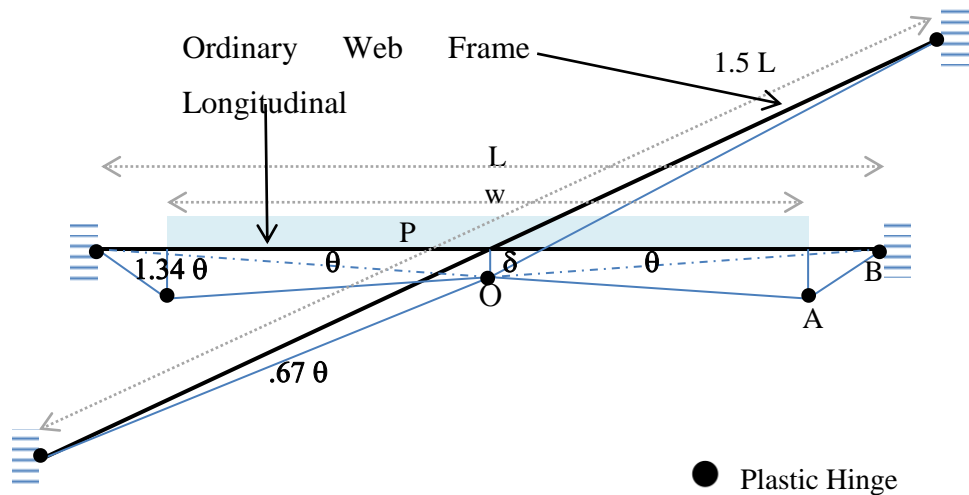


Figure 5-11: 2nd Collapse Mechanism for single longitudinal frame

Then after having an observation from the deformation pattern from the whole grillage (Figure 5-8), it is seen that the maximum deformation is not occurring at mid-point. Maximum deformation is in between the fixed support and the ordinary frame. The position of hinge A (Figure 5-11) is assumed that the maximum deformation happens at the end of the load. So then applying energy principle,



External work:

$$W_e = 2Ps \left[\int_0^{b/2} w_{OA}(x) dx + \int_{b/2}^{L/2} w_{AB}(x) ds \right] \quad (5-4)$$

$$w_{OA} = \delta \left(\frac{L}{L+w} + \frac{2x}{w} \left(1 - \frac{L}{L+w} \right) \right) \quad (5-5)$$

$$w_{AB} = \delta \left(1 + \frac{2x-w}{w-2L} \right) \quad (5-6)$$

So, external work

$$W_e = \delta \frac{P.s}{L+w} \left(wL + \frac{w^2}{2} + \frac{(L-w)^2}{2(w-2L)} \right) \quad (5-7)$$

Taking $L=4.43\text{m}$, $w=4.08$, and length of web= 6.6m we get the angles as shown in Figure 5-11, External Work is,

$$\begin{aligned} W_e &= M_L (2 \times 1.34\theta + 2 \times 2.34\theta) + M_w (4 \times 0.67\theta) \\ &= (7.36M_L + 2.68M_w) \frac{\delta L}{L+w} \frac{2}{L} \end{aligned} \quad (5-8)$$

So the capacity using an ordinary web frame at mid-point of the longitudinal frame be,

$$P = \frac{2(7.36M_L + 2.68M_w)}{s \left(wL + \frac{b^2}{2} + \frac{(L-w)^2}{2(w-2L)} \right)} \quad (5-9)$$



5.7. Analytical Results

Now, the capacity of the longitudinal will be calculated for different cases which were derived earlier.

Case 1: without any support at middle i.e. without taking consideration the ordinary web frame,

1a: All the hinges are pure bending hinge that mean no reduction due to

shear as equation
$$P = \frac{8M_p}{L.b.s.\left(1 - \frac{b}{2L}\right)} \quad (1-35) \text{ capacity is}$$

0.323 MPa

1b: Considering shear reduction as Daley derived, equation (40) capacity is **0.27 MPa**.

Case2: With the ordinary frame at middle,

2a: As 1st collapse mechanism, equation
$$P_1 = \frac{8M_L + 5.37M_w}{LwS\left(1 - \frac{w}{2L}\right)}$$

(5-3), capacity is **2.15 MPa**.

2b: As 2nd collapse mechanism, equation
$$P = \frac{2(7.36M_L + 2.68M_w)}{s.\left(wL + \frac{b^2}{2} + \frac{(L-w)^2}{2(w-2L)}\right)}$$

(5-9), it is **2.13 MPa**.

So I have taken the minimum capacity 2.13 as collapse mechanism principle.

5.8. Abaqus Results

A single longitudinal frame without having any support in middle (case 1, chapter 5.7) span of 4.43m, loading with 4.08m ice load patch, analysis has been done to check the Daley's 3-hinge collapse mechanism derivation as equation (1-40)

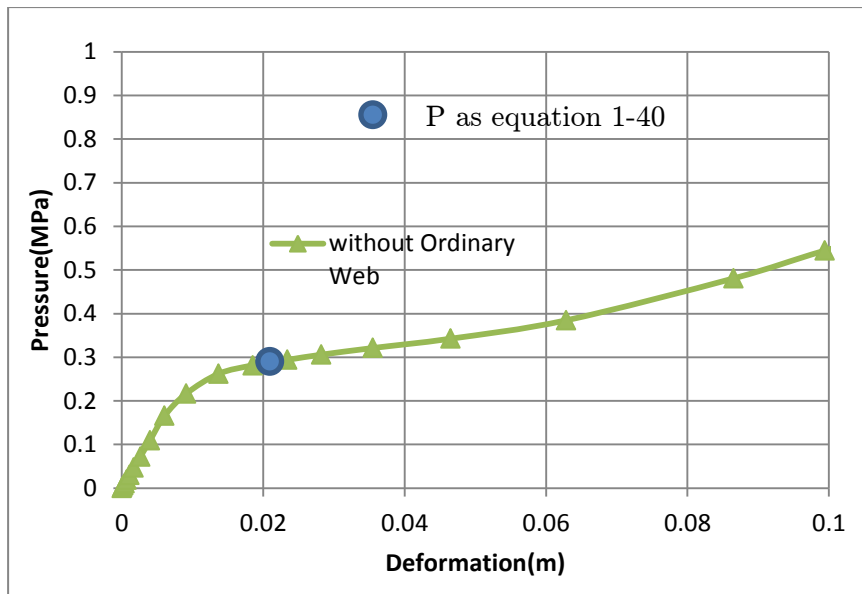


Figure 5-12: Pressure vs. Deformation plot single longitudinal with span of 4.43m (case1)

So it is observed that Daley's 3-hinge capacity of 0.27MPa allowing deformation of 19mm. The limit load according to this plot will be estimated by twice elastic slope method later.

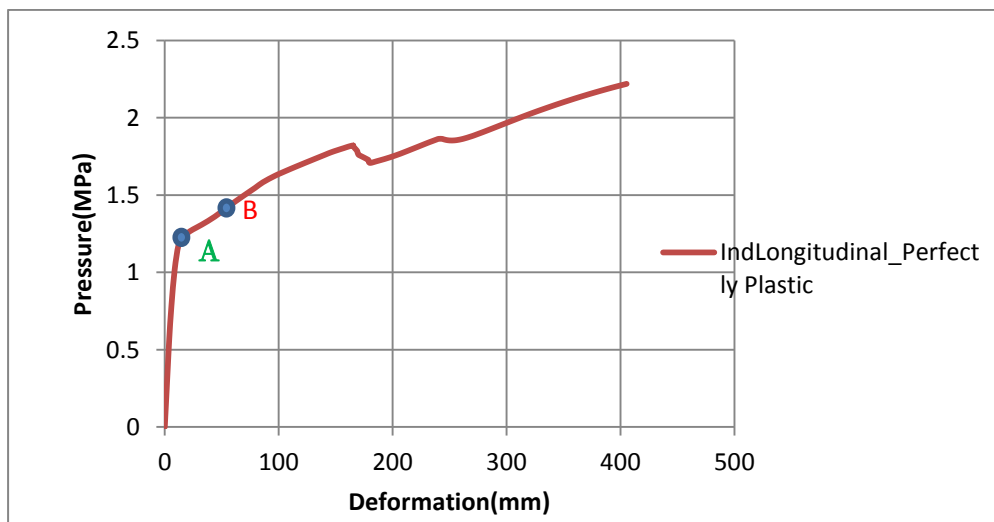


Figure 5-13: Pressure vs. Deformation plot for individual longitudinal at centre.

The above plot is for the mid-point (Figure 5-14, location D) of the longitudinal. Up to 1.1 MPa (point A) it shows elastic behavior with a deflection of 12 m. From the above plot we can see this longitudinal has the

capacity of 1.4 MPa (Point B in Figure 5-13) allowing deformation of 50mm at mid-point of the longitudinal. But from Figure 5-14, the maximum deflection of 81mm is occurring at location E. So it can be said that the 2nd collapse mechanism can't present the actual collapse nature. The collapse load founded using 2nd model is 2.13MPa, which is so much to allow.

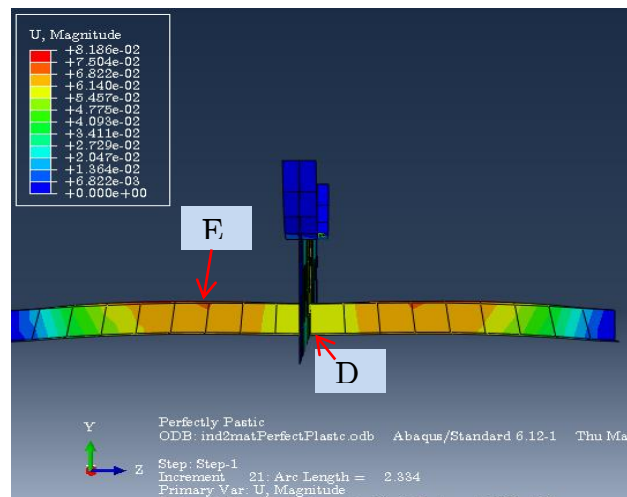


Figure 5-14: Deformation of longitudinal at 1.4 MPa load

But normally it is expected that the analytical value should be higher than real value. Because for analytical calculation it was assumed that all hinges are pure bending moment hinge but at the longitudinal end moment will be reduced due to shear created, has been shown in Figure 5-15 and the capacity will be lower. So the assumption behind the analytical model formed and the position of hinge should be modified. Deformation contour plot for different load will be found at Appendix.

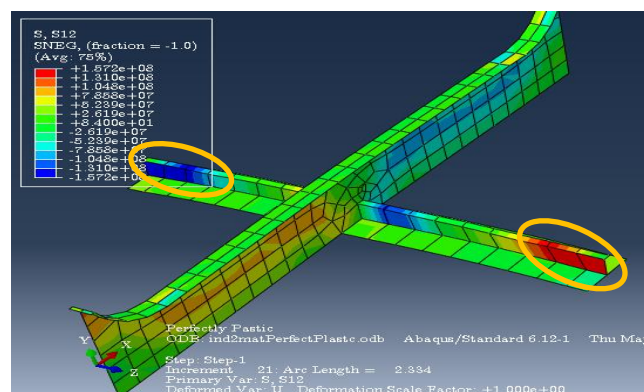


Figure 5-15: Shear Stress in 1.4MPa.

6. Analysis of a large part of the ship side

The large part has been taken the large part is modeled by considering a grillage of 1/2-1-1/2 span (Figure 6-1) in both longitudinal and transverse direction. The half span in both directions has been taken so that we can get a better effect from adjacent structure.

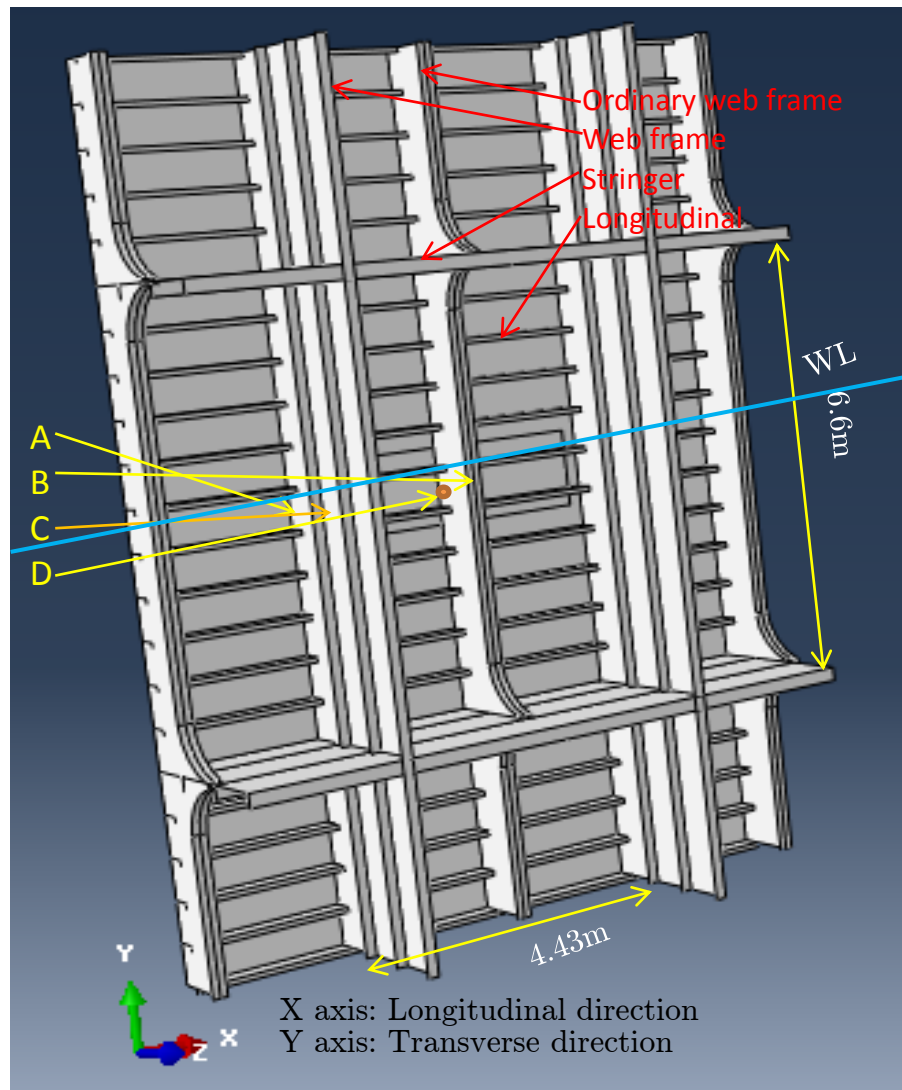


Figure 6-1: Side Structure Abaqus model

The letters A, B, C, D indicated in above figure will be used in further work to denote different location in structure.

6.1. Boundary conditions

Selecting boundary condition for this large part is a difficult issue which will represent that structure has a well connection with adjacent structure. Before applying boundary condition it is necessary to know the hierarchy of load transfer. The load transfer from ice load to this regarding large side part is shown below:

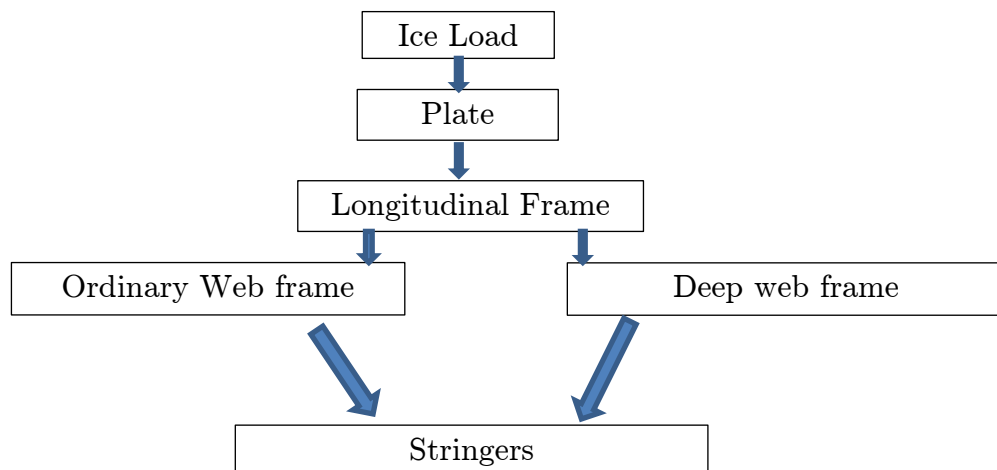


Figure 6-2: Load transfer hierarchy

Another factor to consider is the strength of adjacent structure. For this case stringers and transverse web frames are the heaviest part compared to other members.

Two alternative boundary conditions have been applied to the end of web and stringers.

BC 1: All the stringers and web ends are fixed

BC 2: All the stringers end fixed. Main web and ordinary web ends are symmetric; $U_y = U_{R_x} = U_{R_z} = 0$

For both alternative, same boundary condition have been applied for the plate edges, (see Figure 6-1)

For longitudinal(x-direction) edge: $U_y = U_{R_x} = U_{R_z} = 0$

For transverse(y-direction) edge: $U_x = U_{R_y} = U_{R_z} = 0$

Boundary condition is shown simply below for longitudinal direction plate edge:

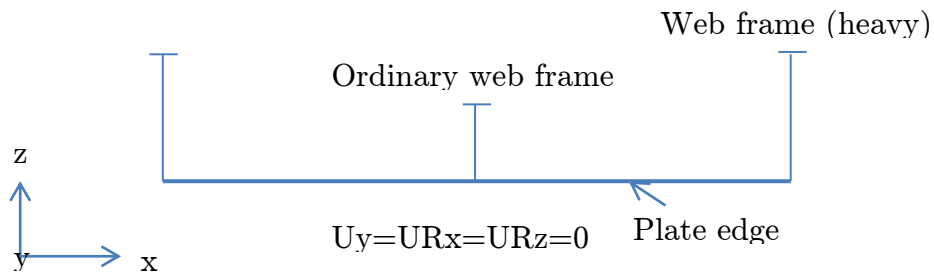


Figure 6-3: Boundary condition for plate edge in longitudinal direction

Symmetric boundary condition creates the support given by adjacent structure. From figure above, adjacent plating in y-direction will restrict to deform this plate edge. So in that direction displacement (U_y) has been kept zero. The adjacent plate will also restrict this edge to rotate about x-axis (U_{R_x}) and z-axis (U_{R_z}).

6.2. Loading

As stated before, this model is intended to assess under IACS polar class 7, the load and the load patch dimensions are applied as calculated in Table 5.

	Ice Load(MPa)	Patch height(m)	Patch width(m)
PC7	3.301475	1.135341	4.087227

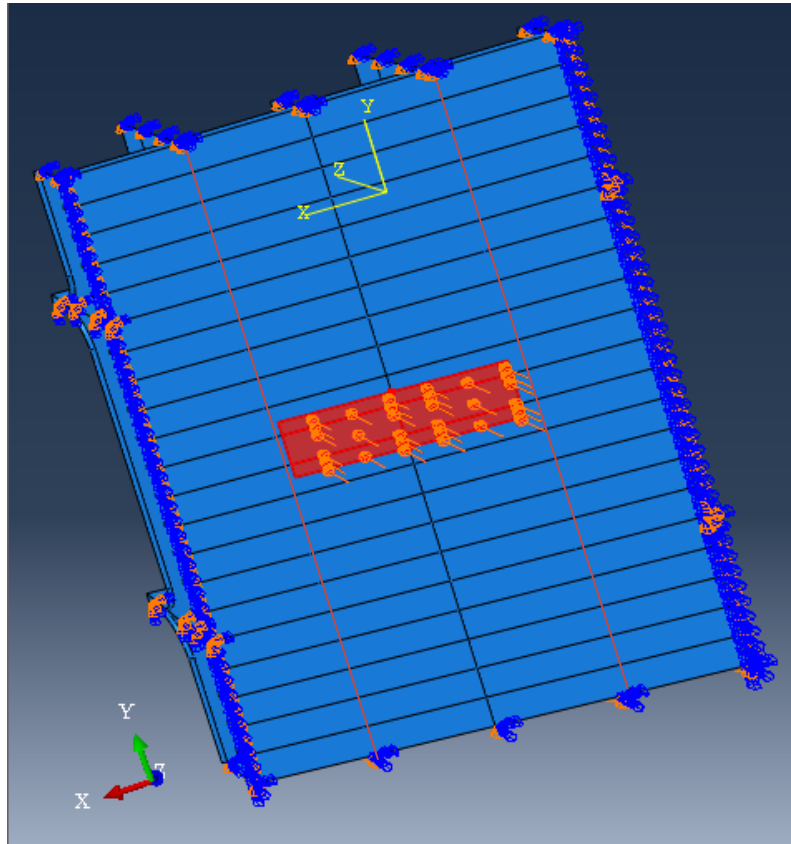


Figure 6-4: Loading on a large side part

The load patch height has covered two longitudinals. The load is applied symmetrically in both directions. The load is applied to positive z-direction.

6.3. Meshing Technique

This part is meshed with Abaqus predefined automatic mesh technique where I've set the average mesh size and element type as shell quad element. Abaqus did the rest of the meshing work automatic. That's why there was no control on meshing specially for critical location and therefore very coarse and un-uniform mesh has been found for this structure (see Figure 6-5, Figure 6-6). The loading area is also not uniformly meshed.

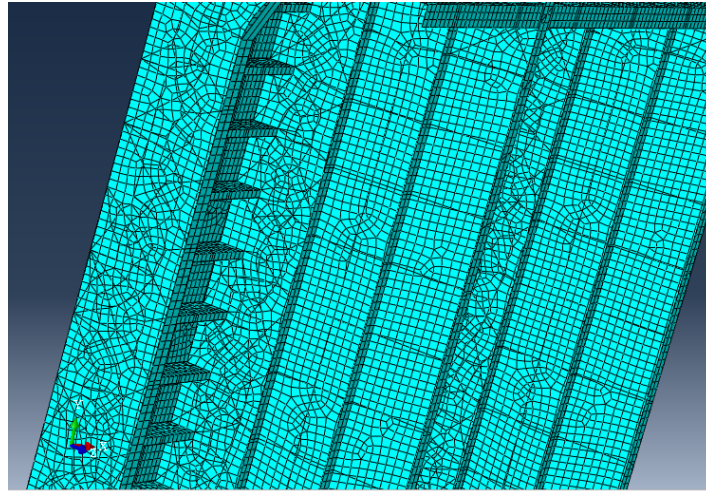


Figure 6-5: Meshing of the model

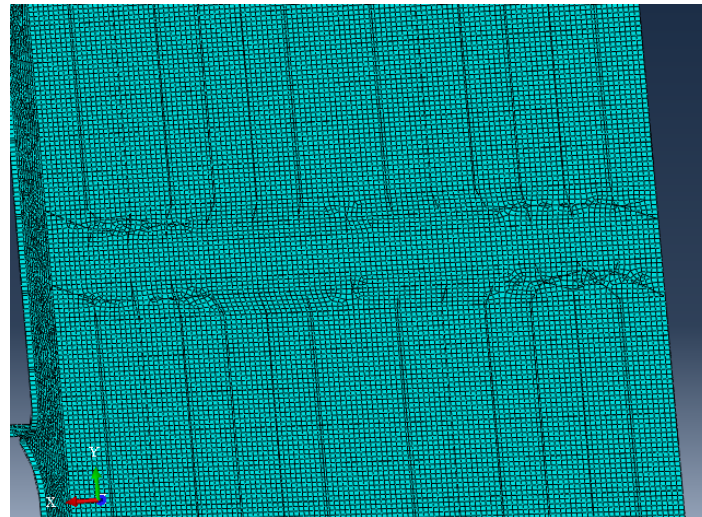


Figure 6-6: Mesh in loading area

6.4. Abaqus analysis result

The whole grillage part has been analyzed with many alternatives like, different boundary condition (BC1 and BC2, stated in chapter 6.1), different plastic property of the material.

6.4.1. Comparing boundary condition

The whole large part has been analyzed for two boundary conditions as described in chapter 6.1. Abaqus result is shown below:

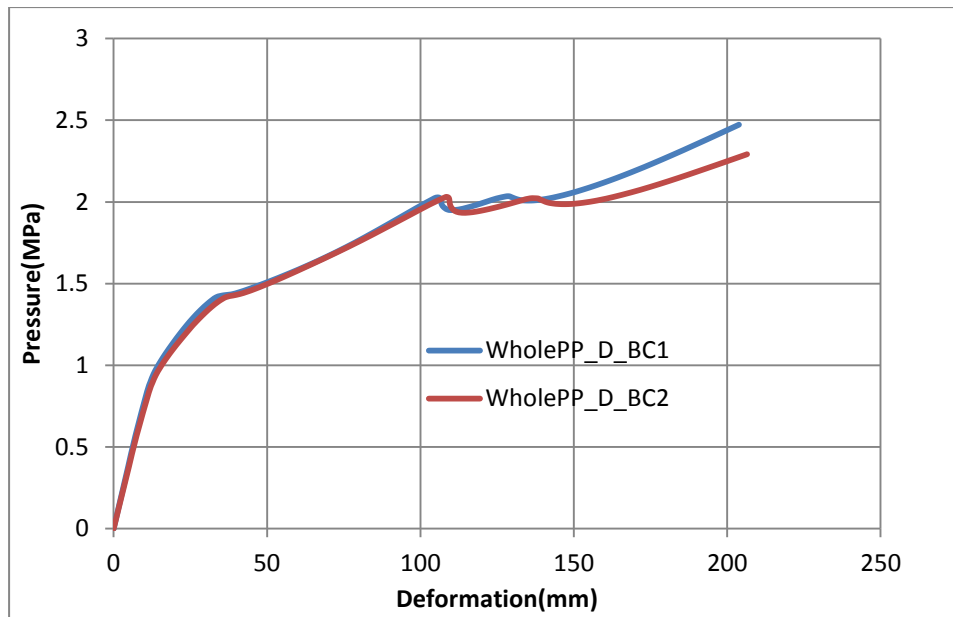


Figure 6-7: Deformation difference between two boundary conditions

[Plot legend meaning: WholePP_D_BC1: whole grillage, perfectly plastic material with boundary condition 1, point location 'D' (see Figure 6-1)]

This plot has been drawn for position 'D' for both boundary conditions. From the above plot, two curves are showing so close nature. That means during calculation of a large part; when pressure is local, far from the applied boundary condition; these two different boundary conditions don't have so much effect in deformation. For the other locations, we can see the deformation and stress contour plot in Appendix (Figure A-6, Figure A-7) which are showing so close nature for both in all position.

6.4.2. Material comparison

Two assumptions regarding plastic property was considered.

1. Elastic pure plastic material
2. Elastic plasticity with 15% hardening.

Both of the material show approximately same behavior up to 100mm deformation (Figure 6-8). This analysis was done considering boundary condition BC1. For further results, pure plastic material model has been used as this is an assumption for deriving the IACS requirements.

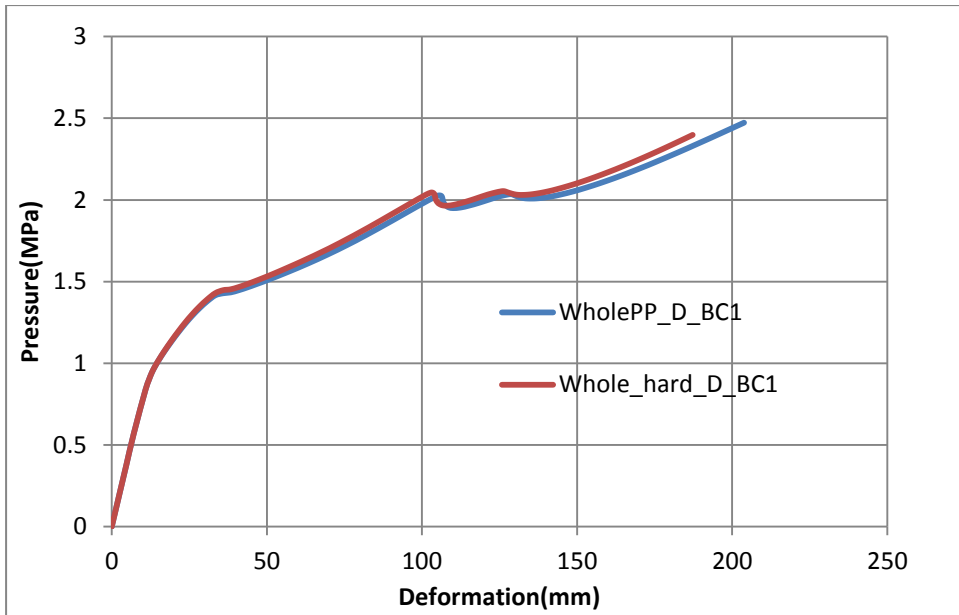


Figure 6-8: Plasticity effect on Abaqus result

6.4.3. Result of whole structure at different positions

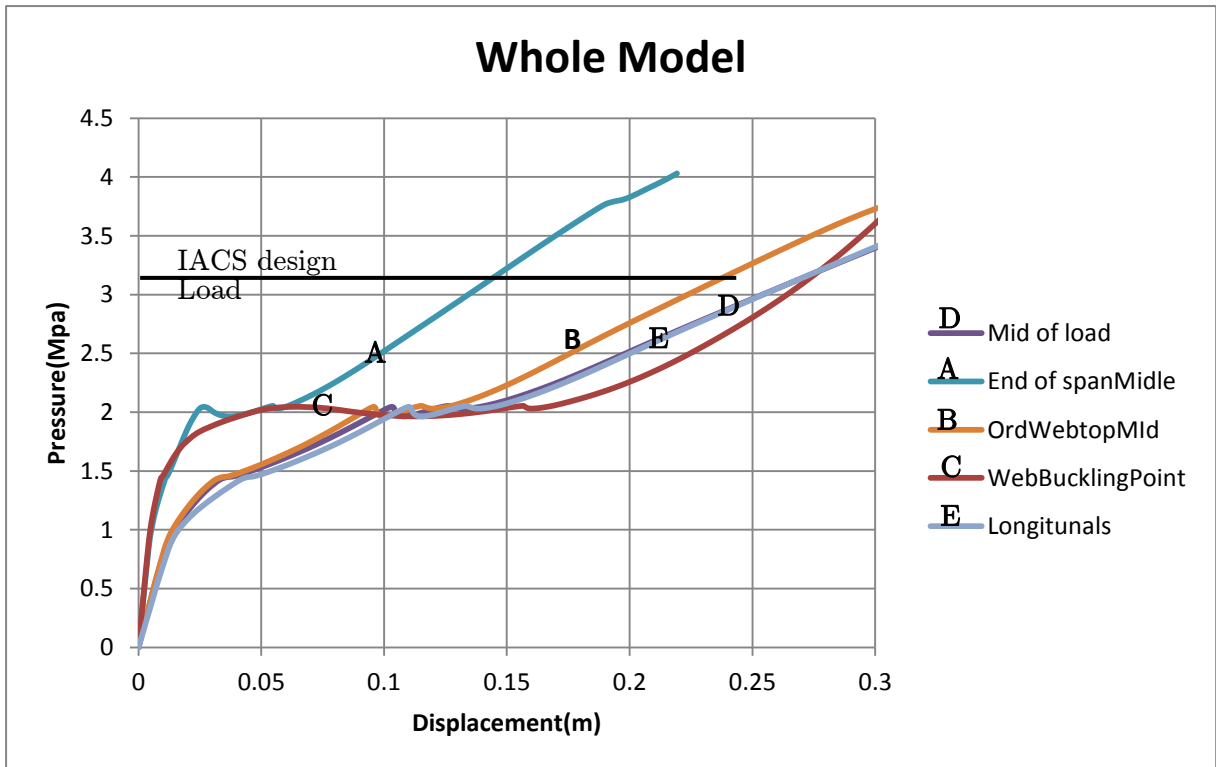


Figure 6-9: Load-deformation plot of whole grillage, at many points

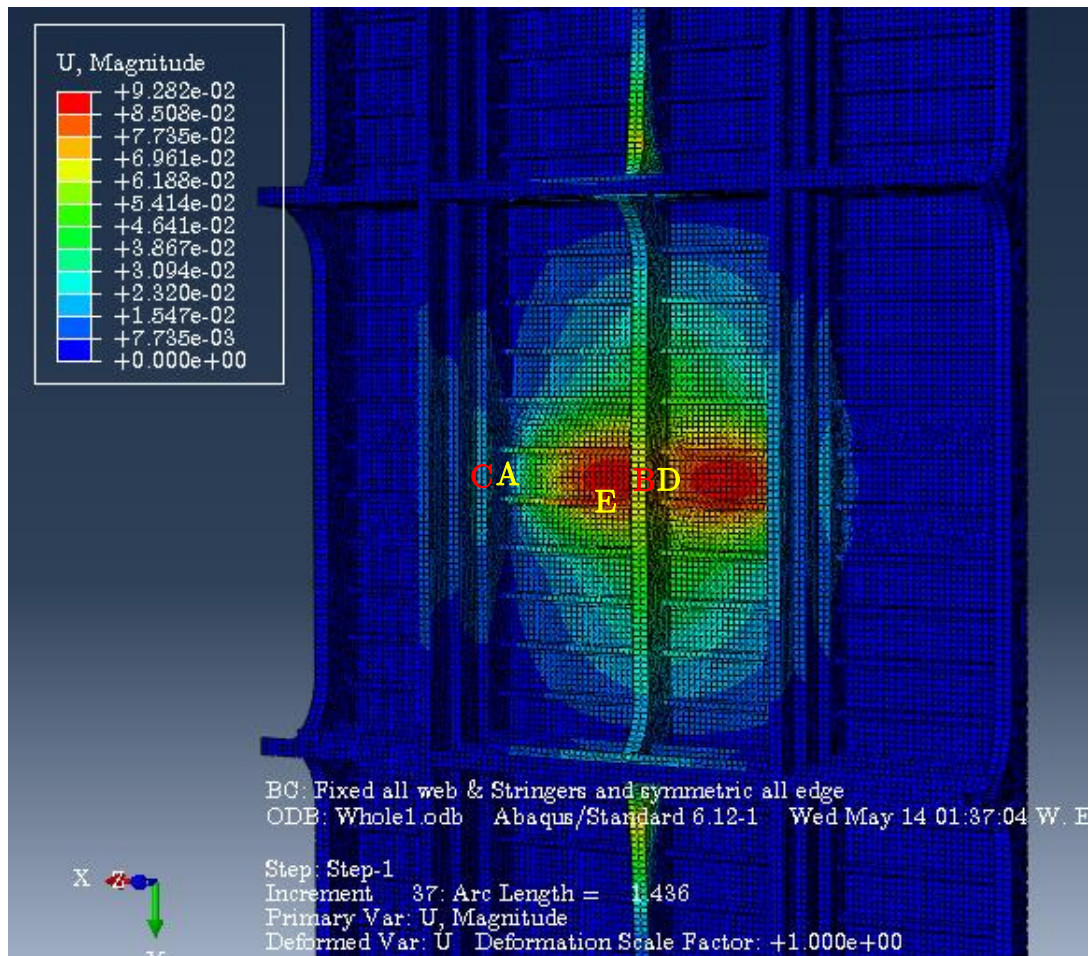


Figure 6-10: Deformation contour plot in 1.7MPa load (showing points for plots in Figure 6-9)

A: this is the intersection point of heavy web and plate. Here structure is showing better capacity of 2.1 MPa, than other points within loaded area with a deformation of 25mm. buckling behavior is found in this position and allowing large deformation with post-buckling.

D: this point is the middle point of loading located at plate and ordinary web intersection. The capacity is considered 1.6 MPa giving deformation of 50mm. It is showing large deformation at a small increase of the load. After reaching at 100mm deflection it shows buckling behavior. Behavior of the point B, E are almost same.

C: this is point located at the web where buckling is occurring. At 2MPa load it starts to buckle. From the curve, it allows large deformation at this load.

From different position analysis it is observed that, as we go far from the load area, we are getting more capacity and at the edge positions the deformations are almost zero though the edges were not fixed. So for design load patch we get much local deformation. See appendix for the deformation plots.

6.4.4. Comparison between whole structure and single longitudinal results

Now, we will compare the results between the longitudinal analyzed individually and longitudinal with whole structure.

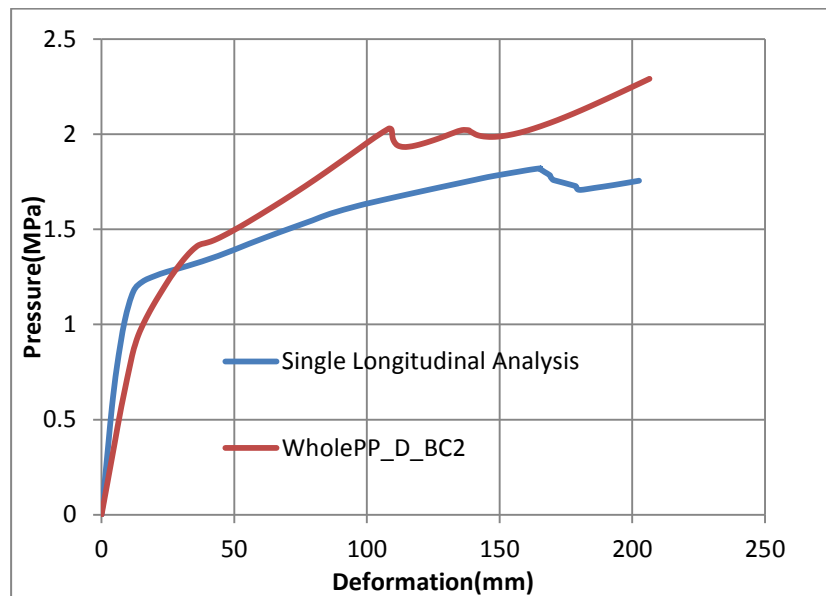


Figure 6-11: Load-Deformation plot for longitudinal (single and in whole structure)

The longitudinal frame is showing higher capacity when it is analyzed in whole grillage model than the capacity when it was analyzed individually. But the longitudinal give higher deformation for whole condition. In whole structure, longitudinal is still showing less capacity than analytically calculated plastic capacity.

- The deformation in whole structure is higher due to line load; Q is double in whole structure analysis as applied pressure is same as individual frame analysis but loaded area is double.
 - This larger deformation might be happening for local pressure effect. The loading in single frame analysis, the load was more uniform through the most of the area of the plate (Figure 5-9).

6.4.5. Introducing additional stiffeners

It is observed that a huge buckling occur at the lower portion of the main web frame which gives the whole part less capacity. Then if we introduce additional stiffeners to the main web of dimension 150x12 at spacing of 600mm then the improvement of capacity of the web increase so much. Before applying the additional stiffener, the web deformation increased infinitely without increasing the load (see figure below).

The capacity at the midpoint (position ‘D’) does not increase much. It is due to the additional stiffener can’t carry the local load at plating and the load transfer through plate, longitudinal to main web frame has not improved by adding the stiffener. So we are getting the same deformation nature at the midpoint of loading. May be capacity can improve by increasing plate thickness.

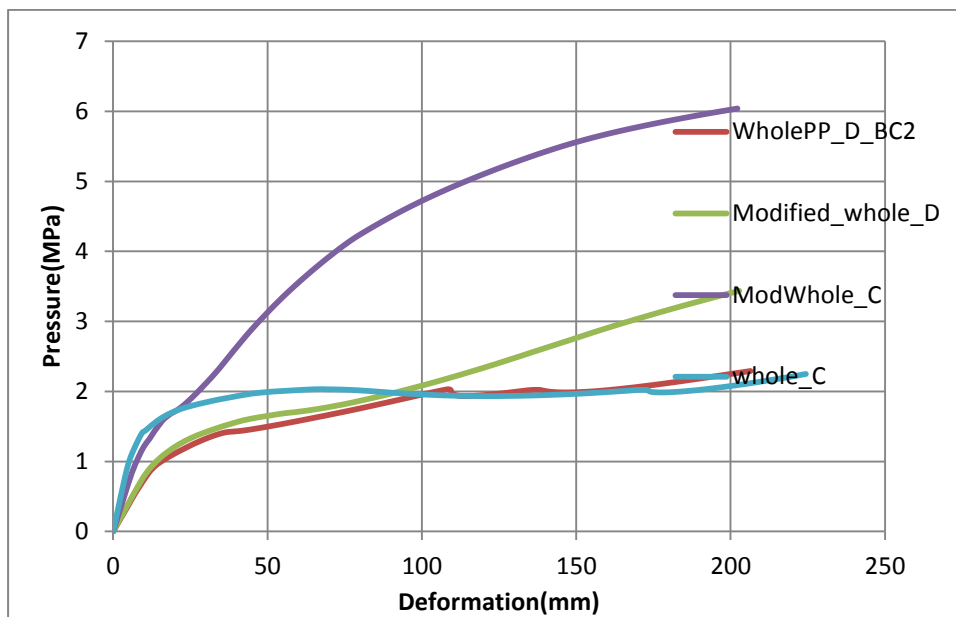


Figure 6-12: Load-Deformation plot for modified grillage

6.5. Assessing limit loads

There are many ways to estimate limit state or capacity. 3-hinge capacity is one of the limit states. If we consider the ideal case, deformation increment will be infinite in 3-hinge capacity load. This ideal case can be obtained by using

elastic-purely plastic plot but in real strain hardening and membrane effect occur. So in real case it is confusing to determine the capacity or limit load. There are many ways to estimate the limit load like twice elastic slope method(TES), tangent intersection method(TI), 0.1% residual strain method etc.

6.5.1. Twice elastic slope method

In load-displacement curve the elastic part is linear. If this linear part slope is $\tan\theta$ then another line is drawn with a slope of $2\tan\theta$. This second line will cut the load deformation in a point and corresponding load is considered as the capacity. This method is used in ASME III [18] and described in the assessment of that code by D G Moffat [19]. But the capacity is often higher than estimated capacity by this method [20]. So using this method will be conservative one.

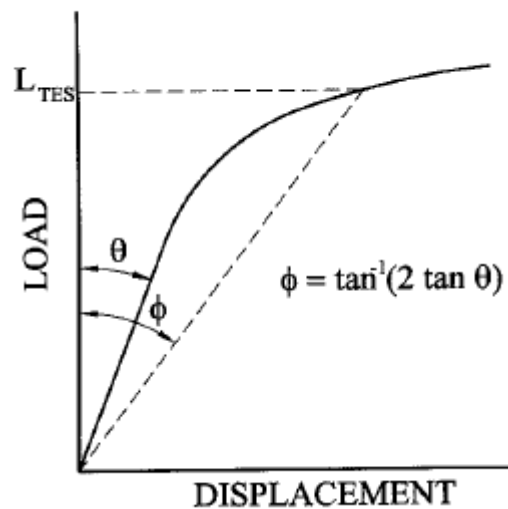


Figure 6-13: Twice elastic slope method [19]

6.5.2. Tangent Intersection Method

This method is the intersection point of elastic tangent and plastic tangent line in the load deformation curve and the corresponding load of that intersection point is considered as the capacity load. This method is recommended in the CEN TC54 draft standard [19]. The confusing fact of this method is to

determine the tangent in the plastic portion. If I see the curves obtained in this thesis work, it is not easy to determine the tangent of the plastic curve.

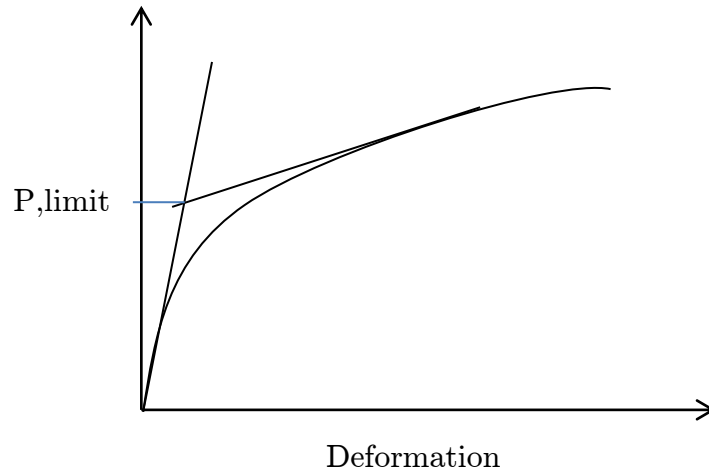


Figure 6-14: Tangent Intersection Method

6.5.3. Limit Loads

So I've used the TES method to determine the limit load for the structure. Limit load for the basic 3-hinge collapse mechanism (Figure 1-19) is obtained as figure below is 0.29 MPa with a deformation of 21mm.

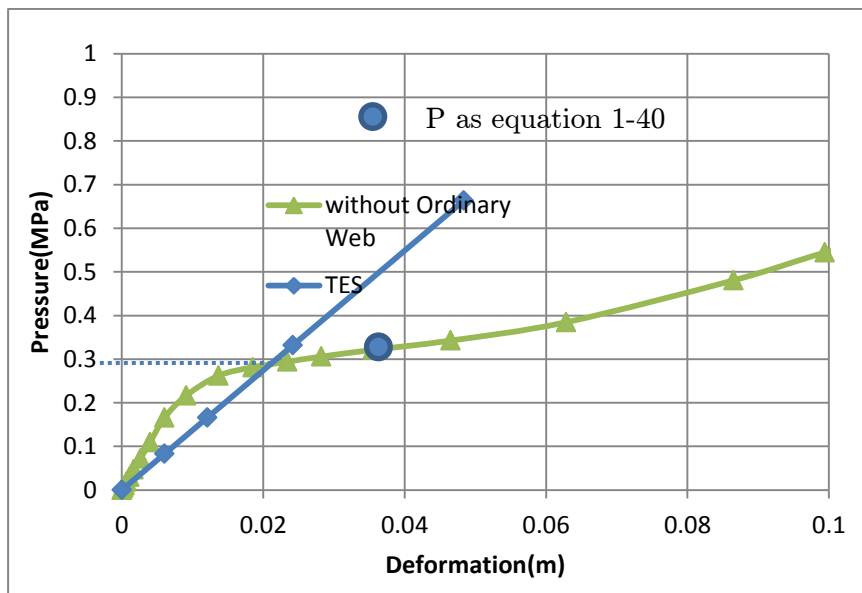


Figure 6-15: Limit load for 3-hinge mechanism

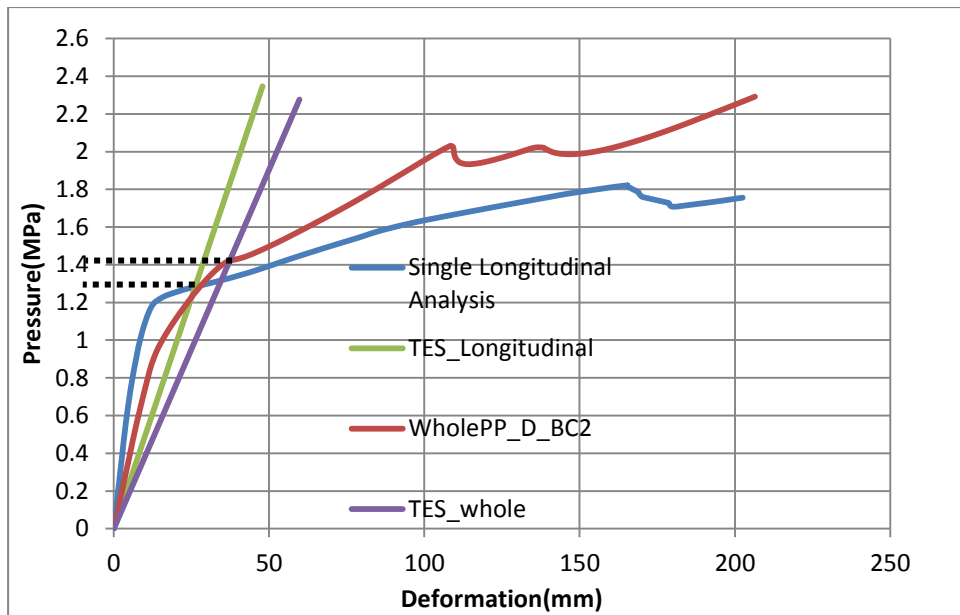


Figure 6-16: Determining Limit Load

Using twice elastic method it is found that, for single longitudinal model the limit load is 1.3MPa and for whole grillage model at position 'D' limit load is 1.42 MPa. Now if we compare with the analytical value, obtained from the collapse mechanism in chapter 5.6, of plastic capacity 2.1 MPa; this value is higher than the value obtained value for both case. May be as stated earlier TES give lower value than actual even then it should not be higher than 2.1 MPa. Because for the analytical calculation, it was assumed the hinges were purely bending hinge but in real the moment is less due to shear effect and membrane effect. Also from the previous discussion, the 2nd collapse model doesn't present the actual collapse model.

Now if we look at the design load for IACS PC7, it is 3.3MPa. The obtained capacities for the frames are so less than the minimum design loads for this size FPSO.

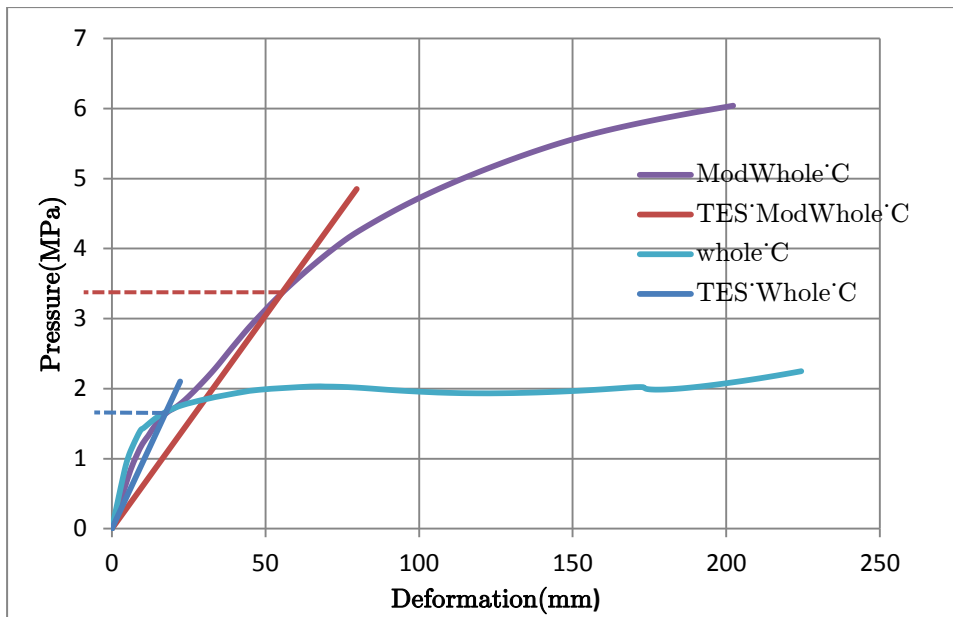


Figure 6-17: Limit loads for web with additional stiffener

So after introducing additional stiffener at web, the capacity has increased so much and it satisfies the PC7 design load and no buckling occur at web but at ordinary web frame buckling occurs.

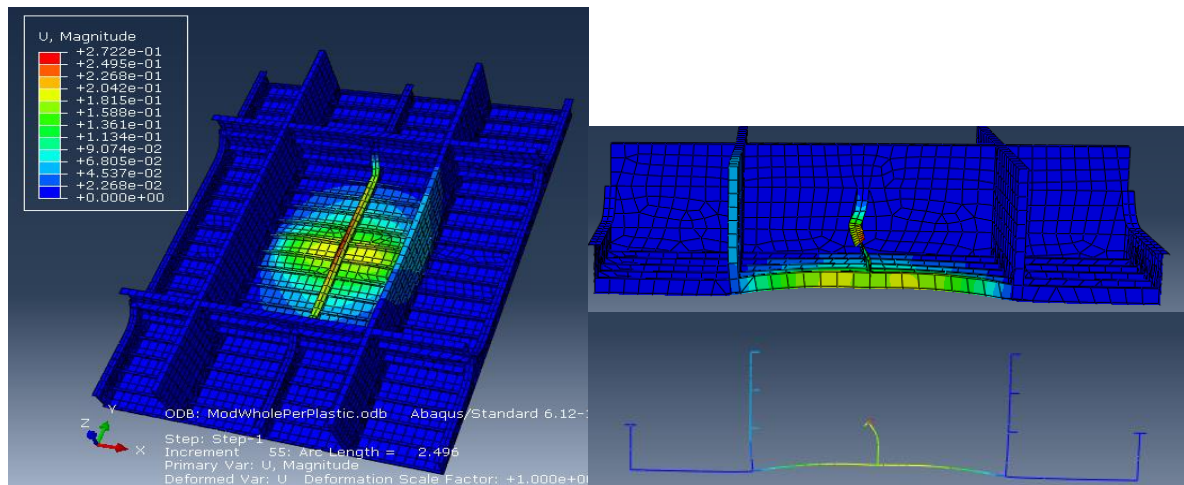


Figure 6-18: Deformation plot of modified grillage

7. Conclusions

IACS framing requirements are based on loading in a single frame and it should be modeled in such a way so that the results of single frame analysis match with the whole large part result within a considerable margin.

From the single frame analysis; for case 1a (see chapter 5.7), the analytical result gives 11% higher value and for case 1b, analytical gives only 6% lower value than simulation result. So considering only pure bending moment give overestimated capacity value but when considering shear and neglecting membrane effect give conservative value within an acceptable margin.

Case 2, simplified single longitudinal frame collapse model of regarding FPSO, gives 62% higher value than simulation limit load. This big difference is inconsiderable, so the assumption of not taking shear effect is not permissible to present a real model. This result has drawn a demand to make a modified model.

From Abaqus result, single frame analysis gives less capacity than whole grillage analysis. But for whole grillage initial displacement is higher than single frame analysis. It is may be due to local deformation. So in single frame analysis local deformation has to be treated may be by considering peak pressure factor (PPF).

Observing all the limit loads, it is clear that this whole part is not satisfying the design ice load of the lightest IACS Polar Class 7. Capacity, within the loaded area or close to loaded area, is maximum 2MPa which is much less than the IACS PC7 average ice patch load, 3.3 MPa. In addition, the minimum shear area requirement is double than the actual shear area of the longitudinal. The plate thickness is also less than the PC7 requirement. The structural stability requirements also don't go with the dimension of web and stringer. The capacity doesn't increase even after introducing additional stiffener at web frame except web frame. So it could be said that this FPSO doesn't comply with IACS PC7. But before giving a certain comment it should be mentioned that, this FPSO is under DNV class but other information i.e. exact DNV polar

class identification, is not investigated. Double hull, as shown in drawings (see appendix, Figure A-1), had also not been considered. So, further analysis by considering double hull or whole FPSO and a quantitative study of DNV polar class are necessary to make a certain comment regarding validity of this FPSO.

8. Recommendation for further work

- A deep comparative study of IACS UR with other classification society is suggested. Especially a brief study of DNV polar class could give this thesis work a better dimension.
- To understand the ice loading well it is recommended to work with energy models, including material models of ice. Then it can bring some arguments on IACS ice load calculation.
- Validity of IACS polar codes for a moored ship/FPSO is further to be assessed.
- Finding a compatible collapse mechanism model for the regarding single longitudinal combined with an ordinary web frame at middle, is the immediate demand to be matched with NLFEM results.

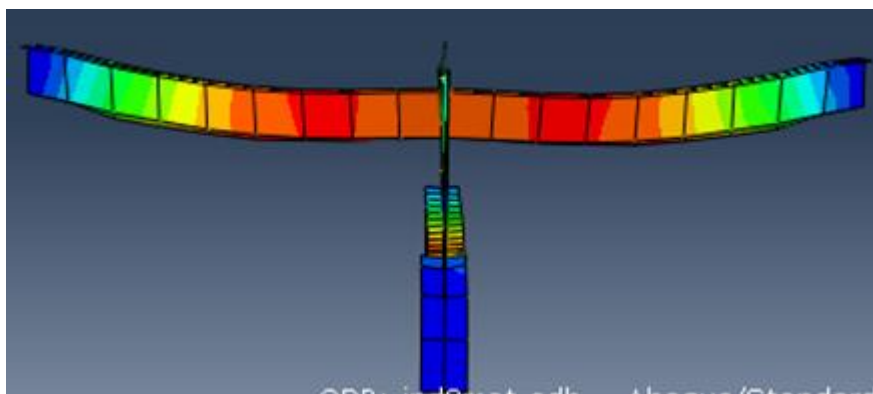


Figure 8-1: Deformation of single longitudinal

After having a good observation from the real deformation, the position of hinge 'A' showed in Figure 5-11 is not positioned correctly, observation for 2nd model was not correct. So another model could be proposed as follows in Figure 8-2. The location of hinge 'A' can be found by maximizing the external work with respect to distance 'a'.

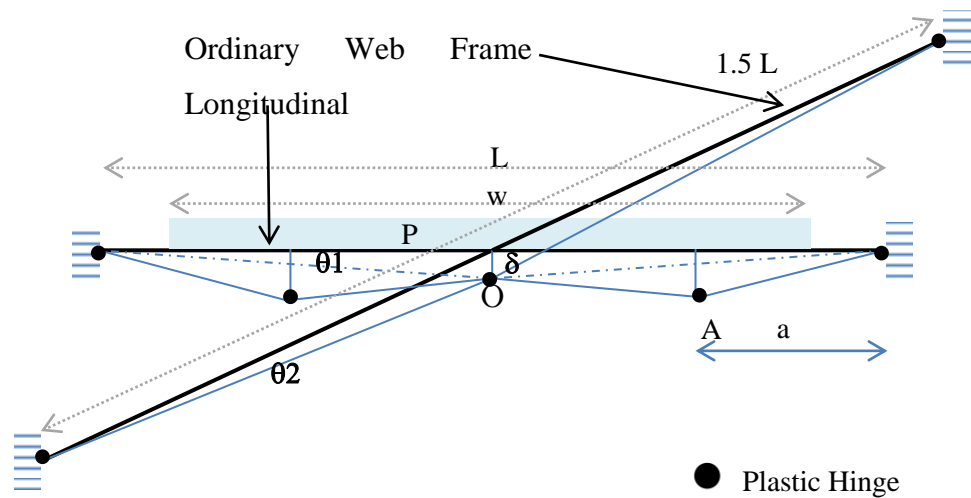


Figure 8-2: 3rd collapse mechanism for longitudinal frame

Assumption also has to be modified. The above model with taking the shear effect on bending can give a good analytical model for regarding FPSO.

- During FEM analysis cut-outs in the web frames were neglected. In addition, intersections of members were not well defined. Meshing of the model should be treated more precisely. So more details analysis is recommended.
- Introducing modified plate thickness, framing dimensions to this FPSO as IACS PC7 requirements and verifying the capacity with regarding design ice load can give a better review of IACS UR.
- This thesis work has motivated to analysis the full detailed FPSO.

Bibliography

1. IACS. *Requirements concerning POLAR CLASS*. 2011.
2. Amdhal, Jorgen. *Compendium, TMR 4205 Buckling and Ultimate Strength of Marine Structures*. Trondheim, Norway : Marine Techonlogy, NTNU, 2007.
3. Daley, C. *Backgrounds Notes to Design Ice Loads: prepared for IACS Ad-hoc group on Polar class ships transport Canada*. 2000.
4. Daley CG, Kendrick A. *Derivation and use of formulations for framing design in the polar class unified requirements*. 2000.
5. Appolonov, Nesterov, Paliy, Timofeev. *A system of forming fundamental engineering solutions on assurance of ice strength and safe ship service in Russian Arctic and freezing seas*. s.l. : Arctic Shipping, 2007.
6. Ehlers, Soren. TMR 4565, Specialization Course. *Sustainable Arctic Sea Transport*. s.l. : Norwegian University of Science & Technology, 2013.
7. Claude Daley, Kaj Riska. *Conceptual Framework for an Ice Load Model*.
8. Amdhal, Jorgen. *STATIC RESISTANCE OF STIFFENED PLATES TO EXPLOSIONS*. s.l. : FABIG Newsletter, 2004.
9. Søreide, Tore H. *Ultimate Load Analysis of Marine Structures*.
10. Mustapha, El Jaaba. *Structural resistance of polar ships to ice loading*. s.l. : Department of Marine Technology, Norwegian University of Science and Technology, 2013.
11. Daley, C.G. *Derivation of plastic framing requirements for polar ships*. s.l. : Faculty of Engineering and Applied Science, Memorial University, St. John's, Canada A1B 3X5, 2002.
12. Arctic Design. *Ice Engineering*. [Online]
<http://www.offshoremoorings.org/Moorings/2009/Group02'Prabhakar/OffshoreMooringsWEBSITE25sept2009/Ice`Vaning.htm>.

13. White Rose Oil Field. *Wikipedia*. [Online]
http://en.wikipedia.org/wiki/White_Rose_oil_field.
14. *Hot Rolled Shipbuilding profiles*. s.l. : Rukki Profiler, 2006.
15. **Moan, T.** *Compendium: Finite Element Modelling and Analysis of Marine Structure; Chapter-12*. s.l. : Marine Technology, Norwegian University of Science & Technology.
16. *Abaqus 6.12; Abaqus documentation*. s.l. : Simula.
17. **Abraham, Jacob.** *Plastic Response of Ship Structure Subjected to Ice Loading*. s.l. : Faculty of Engineering and Applied Science, Memorial University of Newfoundland, September 2008.
18. *ASME Boiler and Pressure Vessel Code, Sec. III, Division 1, Subsec. NB, Sec. NB-3213*. s.l. : American Society of Mechanical Engineers, New York, 1995.
19. *An assessment of ASME III and CEN TC54 methods of determining plastic and limit loads for pressure system components*. **D G Moffat, M F Hsieh, M Lynch**. s.l. : SAGE, Jan 1, 2001.
20. **Gerdeen, J C.** *A critical evaluation of plastic behaviour data and a unified definition of plastic loads for pressure components*. s.l. : American Society of Mechanical Engineers, New York, 1979.
21. **IACS.** *Unified Requirements for Polar Ships, PS1–Polar Ship Structures, Draft Requirements*. 2001.
22. **Beghin, D.** *Ultimate Strength of Laterally Loaded Stiffeners, Discussion Paper to IACS Ad-hoc Group*. 1999.



A. Appendix

Matlab script

For finding the average pressure and design ice load patch dimensions:

```
function []=IACS_requiremntns()
%%%%%%POLAR CLASS
CONSTANTS%%%%%%%%%%%%%%%%%%%%%%%%%%%%%%%%%%%%%%%%%%%%%%%%%%%%%%%%%%%%%%%%%%%%%%%%
CFc=[17.69; 9.89;6.06;4.5;3.1;2.4;1.8];
CFf=[68.6;46.8;21.17;13.48;9;5.49;4.06];
CFd=[2.01;1.75;1.53;1.42;1.31;1.17;1.11];
CFdis=[250;210;180;130;70;40;22];
CFl=[7.46;5.46;4.17;3.15;2.5;2.37;1.81];
AF=[0.7;0.65;0.55;0.55;0.5;0.45;0.45];
corfact=[5;5;5;4;4;3;3];
PPF=1.5;
%%%%%%%%%%%%%%%%%%%%%%%%%%%%%%%%%%%%%%%%%%%%%%%%%%%%%%%%%%%%%%%%%%%%%%%%GIVEN%%%%%%%%%%%%%%%%%%%%%%%%%%%%%%%%%%%%%%%%%%%%%%%%%%%%%%%%%%%%%%%%%%%%%%%%
D=[10;30;60;90;120;150;186.12;200;250];
n=9;
DF = zeros(7,1);
s=0.6;
l=4.43;
sigma=315;
%%%%%%%%%%%%%%%%%%%%%%%%%%%%%%%%%%%%%%%%%%%%%%%%%%%%%%%%%%%%%%%%%%%%%%%%CALCULATION%%%%%%%%%%%%%%%%%%%%%%%%%%%%%%%%%%%%%%%%%%%%%%%%%%%%%%%%%%%%%%%%%%%%%%%%
P=zeros(7,n);
t=zeros(7,n);
b=zeros(7,n);
w=zeros(7,n);
for j=1:n
    for i = 1:7
        if D(j)<=CFdis(i)
            DF(i) = D(j).^0.64;
        else
            DF(i) = CFdis(i).^0.64+0.1*(D(j)-CFdis(i));
        end
    end
end
F=0.36.*CFc.*DF;
Q=0.639.*F.^0.61.*CFd;
w(:,j)=F./Q;
b(:,j)=w(:,j)./3.6;
P(:,j)=F./(b(:,j).*w(:,j));
for i=1:7
    if b(i)>=s
```



```
t(i,j)=500*s*(1/(1+s/(2*1))).*sqrt((PPF*AF(i).*P(i,j))/315
)+corfact(i);
    else t(i,j)=500*s.*((2.*b(i))/s-
(b(i)/s).^2).^0.5.*(1./(1+s/(2*1))).*sqrt((PPF*AF(i).*P(i,
j))/315)+corfact(i);
    end
end
% P(:,j)
% t(:,j)
end
% xlswrite('output.xlsx',P,1,'C3:K9')
% xlswrite('output.xlsx',t,1,'C11:K17')
xlswrite('output.xlsx',w,1,'C61:K67')
xlswrite('output.xlsx',b,1,'C53:K59')
% figure(1)
% plot(D,P);
% xlabel('Displacement(KT)')
% ylabel('Pressure(MPa)')
% legend('PC1','PC2','PC3','PC4','PC5','PC6','PC7',-1)
% figure(2)
% plot(D,t);
% xlabel('Displacement(KT)')
% ylabel('Thickness(mm)')
% legend('PC1','PC2','PC3','PC4','PC5','PC6','PC7',1)
end
```

Provided Drawings

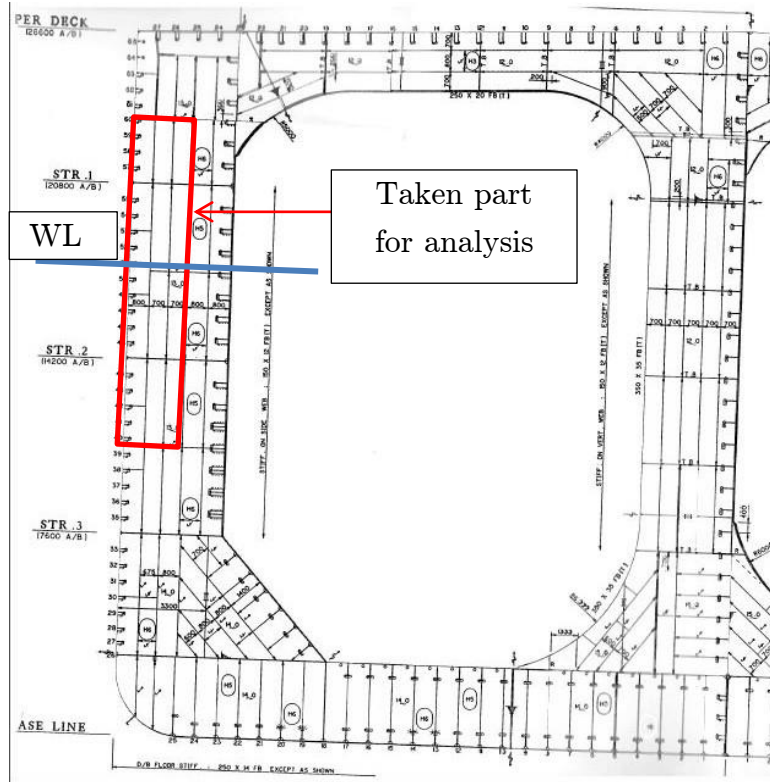


Figure A-1: Drawing of Web frame

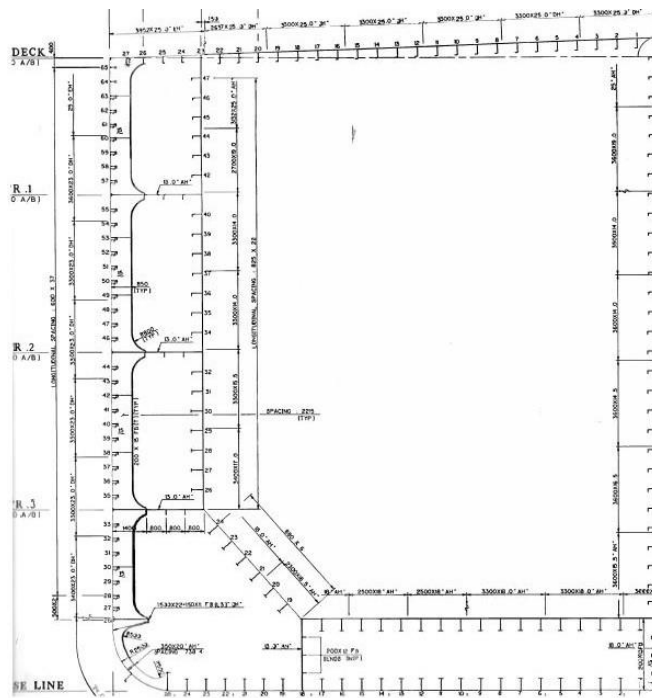


Figure A-2: Drawing of Ordinary web frame

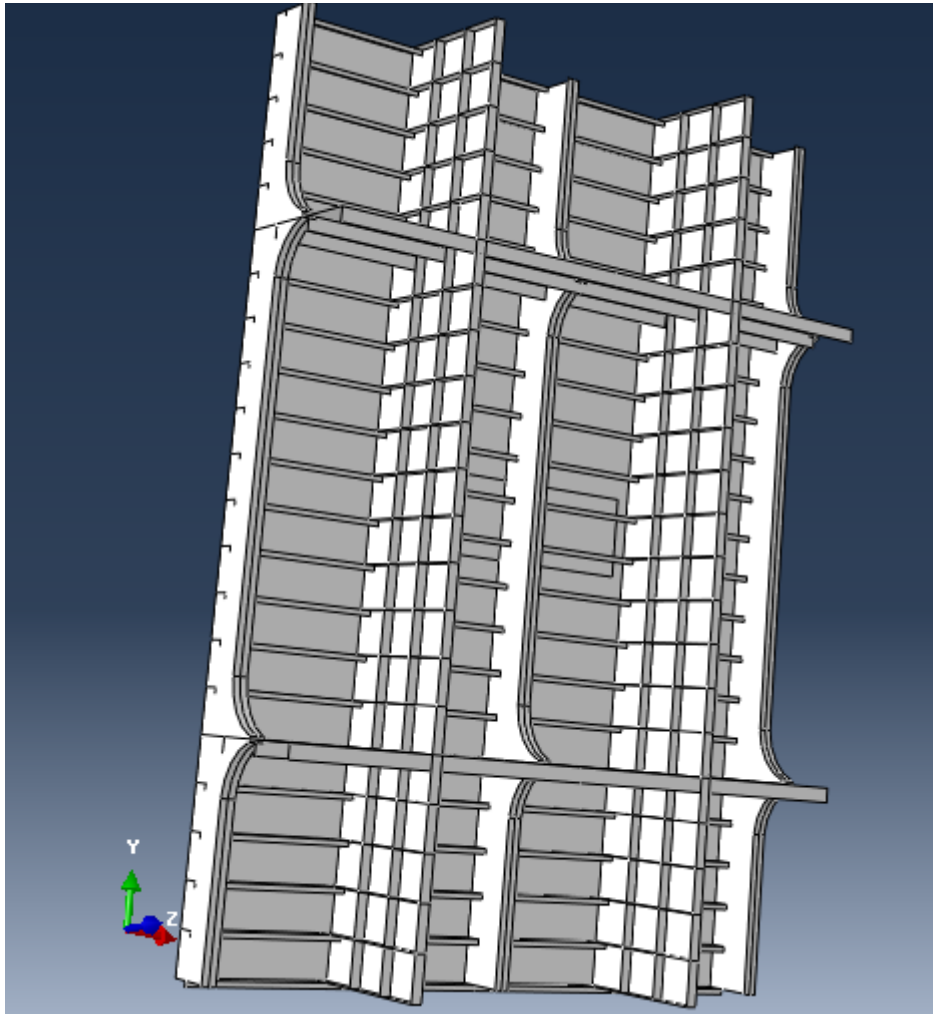


Figure A-3: Modified grillage model

Plots

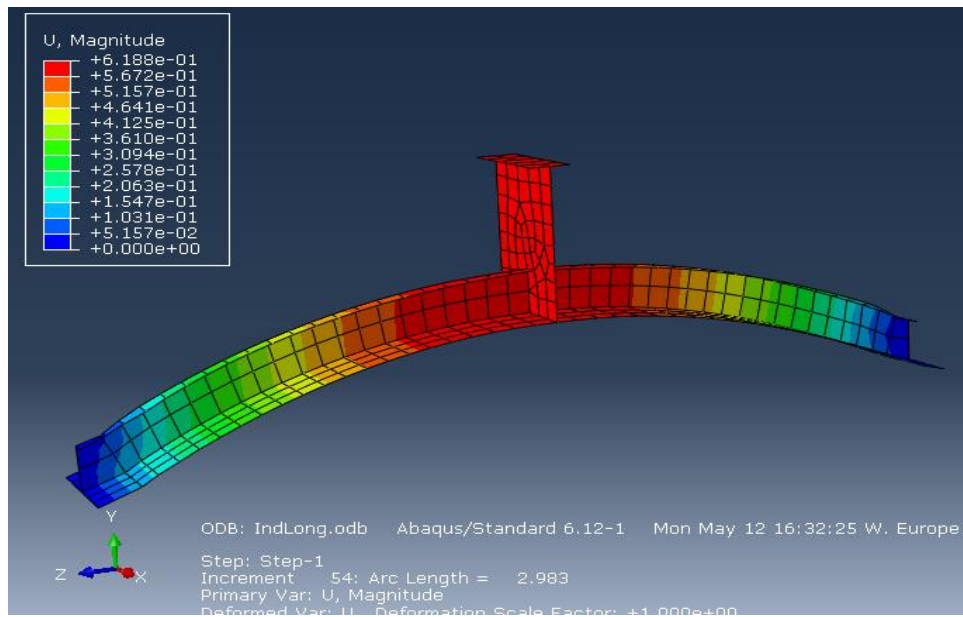


Figure A-4: Displacement contour plot of longitudinal

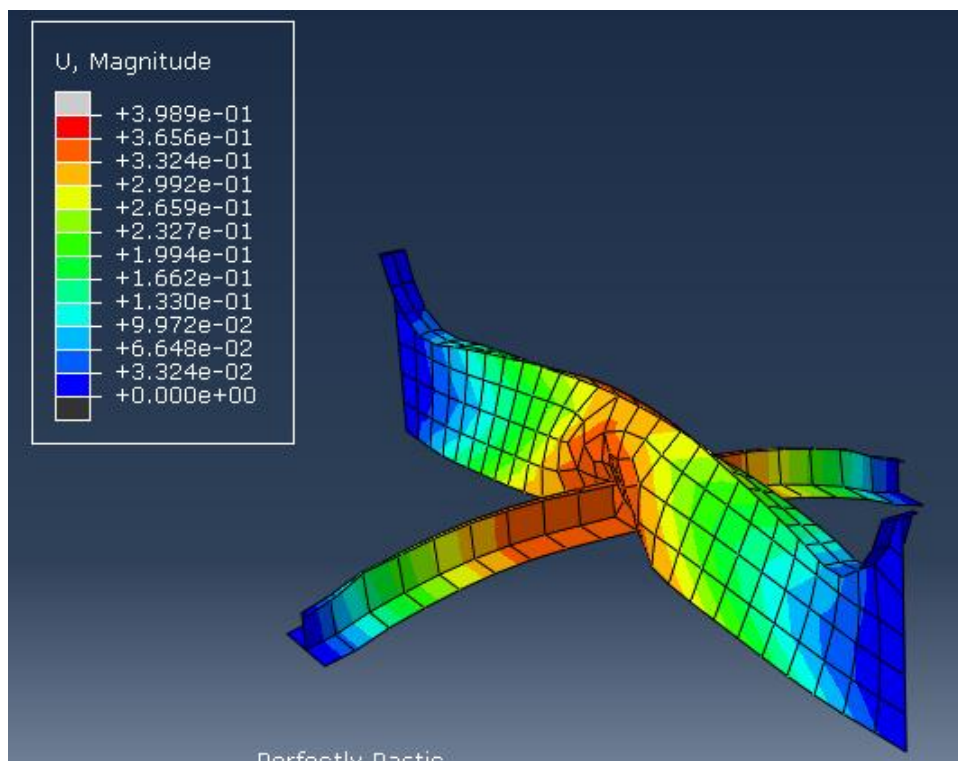


Figure A-5: Deformation at 2.1MPa load

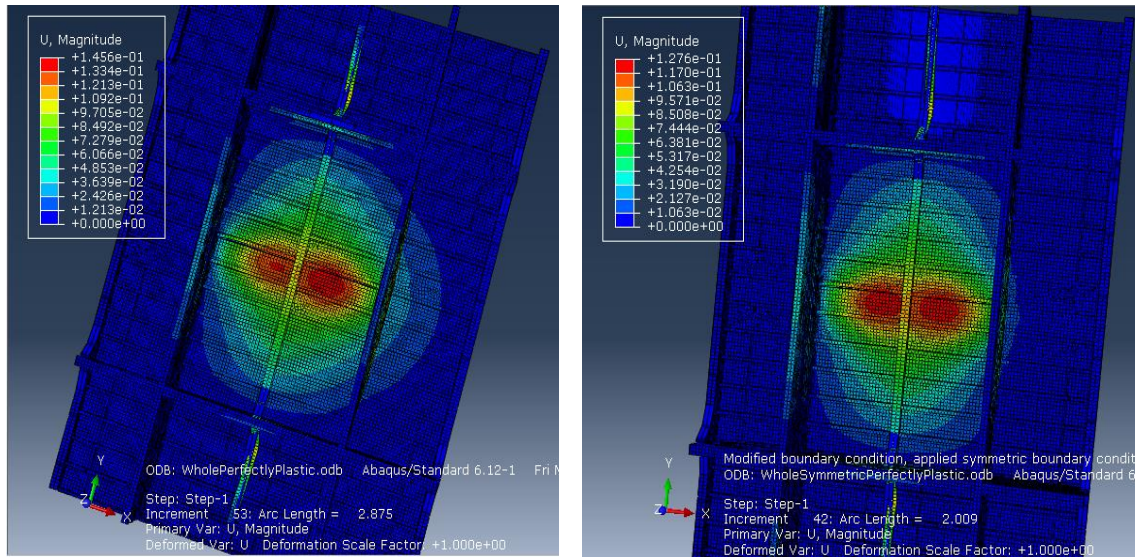


Figure A-6: Deformation contour plot for BC1 and BC2 at 2MPa load

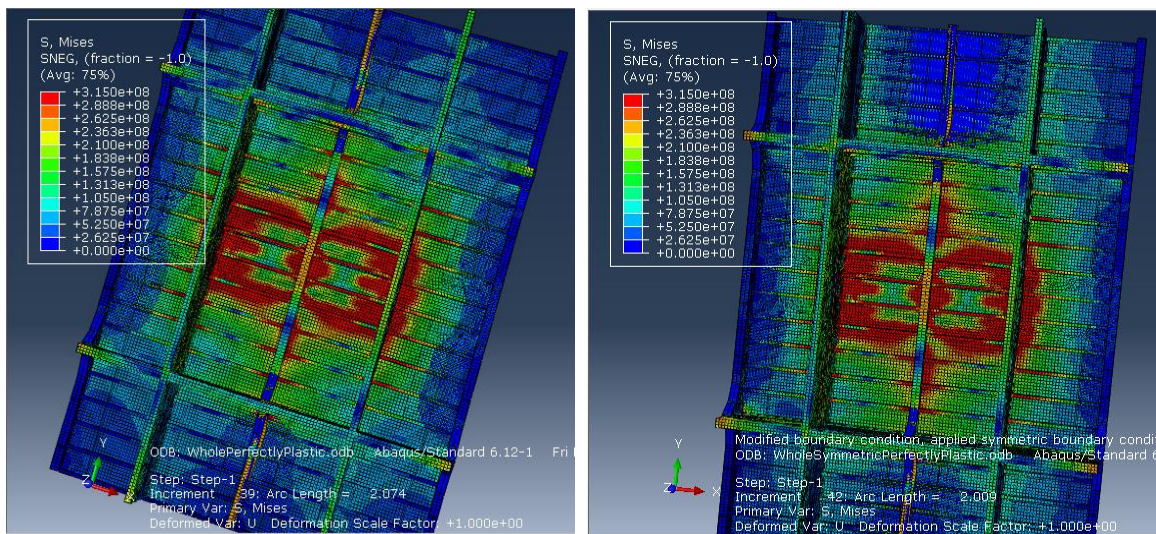


Figure A-7: Stress contour plot for BC1 and BC2 in 2MPa load

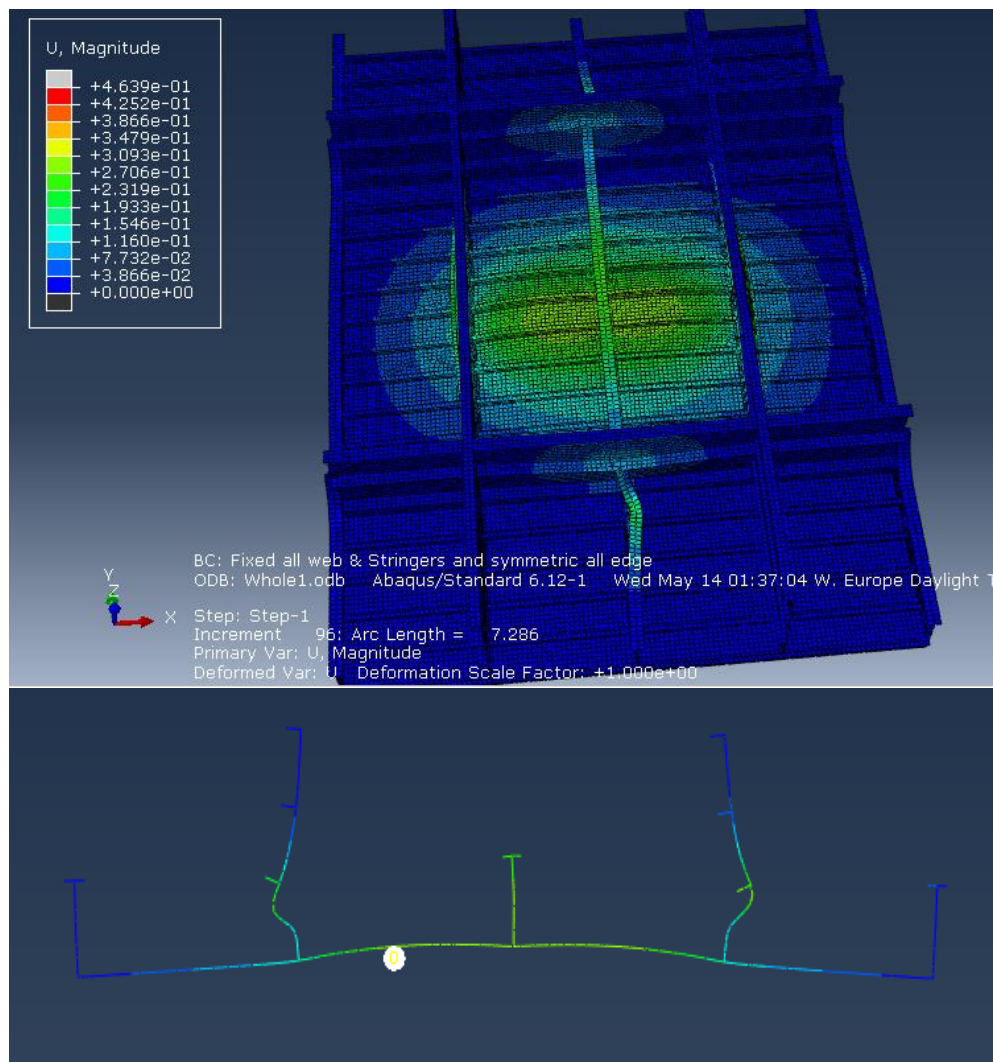


Figure A-8: Deformation at 3.3MPa load

Calculations

Average pressure for different displacements

Displacement	10	30	60	90	120	150	186.12	200	250
PC1	12.34193	14.40661	15.88352	16.81668	17.51184	18.07077	18.62816	18.81776	19.41838
PC2	8.232089	9.609233	10.59434	11.21676	11.68043	12.05324	12.42501	12.55148	12.98386
PC3	5.649599	6.594719	7.270785	7.697948	8.016159	8.272014	8.527931	8.618022	8.917585
PC4	4.557999	5.320505	5.865944	6.210571	6.467299	6.664085	6.868485	6.941598	7.18457
PC5	3.573822	4.171686	4.599352	4.830127	5.004353	5.159397	5.326514	5.386064	5.583218
PC6	2.694691	3.145485	3.402458	3.566139	3.706836	3.830806	3.963362	4.010366	4.16525
PC7	2.276652	2.603374	2.791676	2.94341	3.071603	3.183226	3.301475	3.343173	3.479842

Required Plate Thickness:

1. Span length=2.215m, frame spacing=600mm

Disp.	10	30	60	90	120	150	186.12	200	250
PC1	58.59051	62.89982	65.79526	67.55565	68.8355	69.84622	70.83871	71.17293	72.22067
PC2	47.17538	50.56678	52.84548	54.23089	55.23812	56.03356	56.81464	57.07767	57.96707
PC3	37.13938	39.72377	41.46022	42.51597	43.28352	43.88968	44.48667	44.6947	45.3787
PC4	32.86794	35.18926	36.74897	37.69725	38.38667	38.90591	39.43718	39.62529	40.24341
PC5	28.37243	30.33226	31.64908	32.33424	32.84073	33.2841	33.75458	33.92045	34.46314
PC6	23.07743	24.69189	25.56057	26.09685	26.54807	26.9386	27.34924	27.4932	27.9617
PC7	21.45046	22.73431	23.43554	23.98355	24.43562	24.82164	25.22325	25.36315	25.81568

2. Span length=2.21m, frame spacing=400mm

Disp	10	30	60	90	120	150	186.12	200	250
PC1	42.20638	45.19822	47.20844	48.43063	49.31919	50.02091	50.67312	50.94201	51.66942
PC2	34.28118	36.63574	38.21777	39.17963	39.87892	40.43117	40.94445	41.15606	41.77355
PC3	27.31347	29.10774	30.31331	31.04628	31.57917	32.00001	32.39188	32.55891	33.0338
PC4	24.0422	25.65383	26.73669	27.39505	27.8737	28.23419	28.58259	28.73364	29.16278
PC5	20.92109	22.28175	23.19598	23.67167	24.02331	24.33113	24.63972	24.77293	25.1497
PC6	16.93919	18.06007	18.66317	19.03549	19.34876	19.61989	19.8893	20.00494	20.33021
PC7	15.81243	16.70097	17.18782	17.56829	17.88215	18.15015	18.4137	18.52611	18.84028

3. Span length=4.43m, frame spacing=600mm

PC1	61.98948	66.57211	69.6512	71.52324	72.88426	73.95909	74.95808	75.36995	76.48414
PC2	49.85036	53.45686	55.88008	57.35336	58.42447	59.27036	60.05656	60.3807	61.32651
PC3	39.17782	41.92612	43.77271	44.89542	45.71165	46.35625	46.95648	47.21233	47.93971
PC4	34.69889	37.16744	38.82607	39.8345	40.56765	41.11981	41.65346	41.88482	42.54215
PC5	29.91825	32.00238	33.40272	34.13134	34.66996	35.14144	35.61411	35.81815	36.39526
PC6	24.35084	26.0677	26.99147	27.56177	28.0416	28.4569	28.86955	29.04669	29.54489
PC7	22.62068	23.98595	24.73166	25.31443	25.79518	26.20567	26.60936	26.78153	27.26276

